A general non-hydrostatic hyperbolic formulation for Boussinesq dispersive shallow flows and its numerical approximation

Cipriano Escalante, Tomas Morales de Luna

A general non-hydrostatic hyperbolic formulation for Boussinesq dispersive shallow flows and its numerical approximation

C. Escalante[a], T. Morales de Luna[b]

[a]*Departamento de Matemática Aplicada, Universidad de Málaga, Spain*
[b]*Departamento de Matemáticas, Universidad de Córdoba, Spain*

Abstract

In this paper, we propose a novel first-order reformulation of the most well-known Boussinesq-type systems that are used in ocean engineering. This has the advantage of collecting in a general framework many of the well-known systems used for dispersive flows. Moreover, it avoids the use of high-order derivatives which are not easy to treat numerically, due to the large stencil usually needed. These first-order PDE dispersive systems are then approximated by a novel set of first-order hyperbolic equations. Our new hyperbolic approximation is based on a relaxed augmented system in which the divergence constraints of the velocity flow variables are coupled with the other conservation laws via an evolution equation for the depth-averaged non-hydrostatic pressures.

The most important advantage of this new hyperbolic formulation is that it can be easily discretized with explicit and high-order accurate numerical schemes for hyperbolic conservation laws. There is no longer need of solving implicitly some linear system as it is usually done in many classical approaches of Boussinesq-type models. Here a third-order finite volume scheme based on a CWENO reconstruction has been used. The scheme is well-balanced and can treat correctly wet-dry areas and emerging topographies.

Several numerical tests, which include idealized academic benchmarks and laboratory experiments are proposed, showing the advantage, efficiency and accuracy of the technique proposed here.

Keywords: non-hydrostatic shallow water flows, Boussinesq-type systems, hyperbolic reformulation, breaking waves, path-conservative finite volume methods, well-balanced schemes

1. Introduction

Computational Fluid Mechanics is today one of the most essential tools for the simulation of a multitude of phenomena that take place in our environment related to geophysical flows. These phenomena are of considerable interest since they may affect the population. For instance, the flow that occurs after a dam break, the circulation of bodies in the water, the behavior of atmospheric currents, the evolution of pollutant discharge, erosion and the transport of sediments, the propagation of a tsunami and its impact on a coastal area, among others, are of particular interest.

When modeling and simulating geophysical flows, the Nonlinear Shallow-Water equations, hereinafter SWE, are often a good choice as an approximation of the Navier-Stokes equations. Nevertheless, SWE do not take into account the effects associated with dispersive waves.

In fluid dynamics, dispersion of water waves generally refers to frequency dispersion, which means that waves of different wavelengths travel at different phase speeds. Water waves, in this context, are waves propagating on the water surface, with gravity and surface tension as the restoring forces. As a result, water with a free-surface is generally considered to be a dispersive medium. However, it is well-known that SWE do not take into account the effects associated with dispersive waves. The Stokes linear theory (or Airy wave theory) explains this situation since it states that the speed of wave propagation depends on the depth. More precisely, the phase velocity C_{Airy} is given in terms of the typical depth H, the gravitational acceleration g and the local wavenumber k as

$$C_{Airy}^2 = gH\frac{\tanh(kH)}{kH}.$$

It is a known fact that the phase velocity of SWE is given by

$$C_{SWE}^2 = gH,$$

which is far from the value C_{Airy}.

In recent years, an effort has been made in the derivation of relatively simple mathematical models for shallow water flows that include long nonlinear water waves. To improve the nonlinear dispersive properties of the model, information on the vertical structure of the flow should be included. To do so, the approach used by Boussinesq-type models is to retain some high-order terms in the Taylor expansion of the velocity potential. For instance, this is the approach used in [1], [2], [3], [4], [5], [6], [7], [8], [9], and [10], among others. High-order Boussinesq-type models offer better dispersive properties. The counterpart is that extremely complex systems with high-order derivatives arise (see for instance fifth-order derivatives in [10]). This requires equally complex numerical schemes when solving the equations. Moreover, a large stencil is needed to approximate the high-order derivatives and the development of high-order schemes is not an easy task.

Alternatively, the development of non-hydrostatic pressure models for coastal water waves has been the topic of many studies over the past 30 years. The idea is that, in order to incorporate dispersive effects in SWE-type models, one should retain some vertical information on the structure of the flows. This means that following the usual average process when obtaining SWE, one cannot assume the vertical velocity or non-hydrostatic pressure negligible. Therefore, the pressure is split into a hydrostatic and a non-hydrostatic part. See for instance [11], [12], [13], and [14], among others. The relation between non-hydrostatic pressure models and high-order Boussinesq-type models is not straightforward, although some works show that they are similar. See for instance how in [13] the authors show that the non-hydrostatic model they propose is related to [3], for the case of flat bottom and a modified relation on the pressure terms. Another example is the work [15] where again the non-hydrostatic model is compared to [3] or [16], where a specific quadratic vertical profile for the non-hydrostatic pressure yield equivalence to the Green-Naghdi equations.

The advantage of non-hydrostatic models is that they present only first-order derivatives, which are easier to treat numerically. Moreover, the particular structure of these types of models and their similarities with SWE allow extending many well-known numerical schemes for SWE to non-hydrostatic models as it is done in [17]. One of the drawbacks of non-hydrostatic models is that they do not fall into the class of hyperbolic PDE systems. Moreover, it is required to solve implicit problems that account for the pressure term (see [17]). Implicit numerical schemes for this class of PDEs will lead to solving linear systems at each time step of the numerical scheme that will become the main bottleneck of the algorithm from a computational time point of view. This is done to avoid the restrictive time step that would give an explicit scheme. Moreover, the numerical stencil and the condition number of the underlying linear system to be solved will increase with the order of the scheme.

The first objective of this paper is to establish a link between the most well-known Boussinesq-type and non-hydrostatic models. In particular, we propose a general non-hydrostatic system that allows covering all the classical dispersive systems. This general formulation has the advantage that it will only include first-order derivatives, which are easier to treat numerically. Moreover, as we have said, this would allow adapting different well known numerical techniques similar to the work introduced in [17]. Nevertheless, we will merely establish the equivalence between the two types of systems: Boussinesq-type and non-hydrostatic models. This does not change the nature of the system, which means that the underlying difficulties related to the parabolic nature of the system remain.

Another advantage of this general formulation is that it allows in an easy way to extend the classical Boussinesq systems by including some of the terms that were originally neglected without adding any extra complexity to the system.

The second goal of the paper will be to use the proposed general non-hydrostatic system to present a general numerical approach. The approach is based on a technique similar to the one introduced in [18]. The idea is to propose a relaxation of the system which will cover the original one in the relaxed limit. The relaxed system is hyperbolic and will be solved by employing a high-order finite volume scheme. The advantage is clear, as any numerical technique used for the non-conservative hyperbolic system may be applied. Moreover, the extension to a high-order scheme will be now easier.

The rest of the paper is organized as follows. Section 2 and 3 contain the derivation of the governing equations and the reformulation of classical Boussinesq-type systems respectively; Section 4 and 5 present the hyperbolic ap-
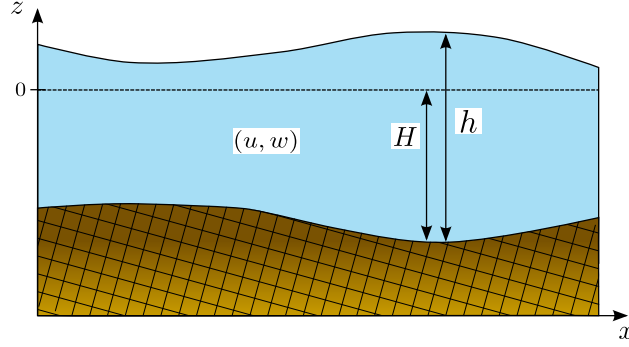
Figure 1: Sketch of the problem considered.

proximation technique and the numerical scheme respectively and Section 6 shows some numerical tests. Finally, Section 7 summarizes the findings of this paper.

2. Derivation of the non-hydrostatic pressure system

In this section, a depth-averaged system derived from Euler equations is presented. In the deduction of the equations, some assumptions will be made on the vertical profile of the velocities as well as the pressure. For the sake of simplicity, we shall consider here the 2D case so that (x, z) will represent the horizontal and vertical coordinates. Nevertheless, everything that is done here can be easily generalized to the full 3D case. In this framework, we consider the 2D Euler system

$$\begin{cases} \partial_x u + \partial_z w = 0, & \text{(1a)} \\[1mm] \partial_t u + \partial_x \left(u^2 + p_T \right) + \partial_z \left(uw \right) = 0, & \text{(1b)} \\[1mm] \partial_t w + \partial_x \left(uw \right) + \partial_z \left(w^2 + p_T \right) = -g, & \text{(1c)} \end{cases}$$

where x and z denote the horizontal Ox and the vertical Oz axis respectively. We consider this system for

$$t > t_0, \ x \in \mathbb{R}, \ -H(x, t) \le z \le \eta(x, t),$$

where η is the unknown water elevation and H is the bathymetry, measured from a fixed reference level and it may vary in space and time. u and w are the horizontal and vertical velocities respectively. The water height is $h = \eta + H$. See Figure 1 for a sketch of the problem. The model is completed with boundary conditions at the free-surface and at the bottom. More explicitly,

$$\begin{cases} w(x, \eta(x, t), t) = \partial_t \eta(x, t) + u(x, \eta(x, t), t) \partial_x \eta(x, t), & \text{(2a)} \\[1mm] p_T((x, \eta(x, t), t)) = p^{atm}, & \text{(2b)} \end{cases}$$

where p^{atm} is the atmospheric pressure, and no-penetration boundary condition is assumed at the bottom,

$$w(x, -H(x, t), t) = -u(x, -H(x, t), t) \partial_x H - \partial_t H. \tag{3}$$

The total pressure p_T shall be decomposed into a sum of a hydrostatic and non-hydrostatic part:

$$p_T = p^{atm} + g(\eta - z) + p, \tag{4}$$

where $p(x, z, t)$ is the non-hydrostatic pressure. Hereinafter, the atmospheric pressure will be supposed to be zero and the non-hydrostatic pressure is assumed to vanish at the free-surface

$$p(x, \eta(x, t), t) = 0. \tag{5}$$

3

In what follows, given a function f, we will denote by $\overline{f}$ its average over the vertical direction z:

$$\overline{f} \equiv \overline{f}(x) = \frac{1}{h} \int_{-H}^{\eta} f(x, z) \, dz.$$

We denote by $\hat{f}$ its deviation with respect to the vertical average:

$$\hat{f} = f - \overline{f}.$$

The integration on the vertical direction z of the incompressibility equation (1a), combined with conditions (2a) and (3), gives the mass equation,

$$\partial_t h + \partial_x (h\overline{u}) = 0. \tag{6}$$

In a similar way, the integration on the vertical direction z of the momentum equation for u (1b) combined with conditions (2) and (3), gives the momentum equation for the depth integrated horizontal velocity $\overline{u}$,

$$\partial_t (h\overline{u}) + \partial_x \left(h\overline{u^2} + \frac{1}{2} g h^2 + h\overline{p} \right) = (gh + p_b) \, \partial_x H, \tag{7}$$

where p_b denotes the non-hydrostatic pressure at the bottom.

The following vertical momentum equation is also deduced by the integration on the vertical direction of the momentum equation for w (1c) combined with conditions (2) and (3):

$$\partial_t (h\overline{w}) + \partial_x (h\overline{uw}) = p_b.$$

Note that given two function f_1 and f_2 we have

$$\overline{f_1 f_2} = \overline{f_1} \cdot \overline{f_2} + \overline{\hat{f_1}\hat{f_2}}.$$

Therefore we get:

$$\partial_t (h\overline{u}) + \partial_x \left(h\overline{u}^2 + \frac{1}{2} g h^2 + h\overline{p} \right) + \partial_x \left(h\overline{\hat{u}^2} \right) = (gh + p_b) \, \partial_x H,$$

$$\partial_t (h\overline{w}) + \partial_x (h\overline{u}\,\overline{w}) + \partial_x \left(h\overline{\hat{u}\hat{w}} \right) = p_b.$$

Using (1a), equation (1c) can be rewritten as

$$\partial_t w + u\partial_x w + w\partial_z w + \partial_z p = 0.$$

Taking the derivative with respect to z on the last equation, one gets

$$\partial_t (\partial_z w) + \overline{u}\partial_x (\partial_z w) + (\partial_z w)^2 = -\partial_z(\hat{u}\partial_x w) - w\partial_{zz} w - \partial_{zz} p.$$

Finally, multiplying by h^2 and using the mass equation (6), we get

$$h\partial_t (h\partial_z w) + h\partial_x (h\overline{u}\partial_z w) + h^2 (\partial_z w)^2 = -h^2\partial_z(\hat{u}\partial_x w) - h^2 w\partial_{zz} w - h^2 \partial_{zz} p.$$

Now remark that, again using the mass equation combined with (1a), we have:

$$h\partial_z w\partial_t h + h\overline{u}\partial_z w\partial_x h = -h^2\partial_z w\partial_x \overline{u} = h^2(\partial_z w)^2 + h^2\partial_z w\partial_x \hat{u},$$

which combined with previous equation gives us:

$$\partial_t \left(h^2 \partial_z w \right) + \partial_x \left(h^2 \overline{u}\partial_z w \right) = h^2\partial_z w\partial_x \hat{u} - h^2\partial_z(\hat{u}\partial_x w) - h^2 w\partial_{zz} w - h^2\partial_{zz} p.$$

Equivalently, using the notation $\xi = -\frac{1}{12} h\partial_x u$, one may write

$$\partial_t (h\xi) + \partial_x (\overline{u}h\xi) = \frac{1}{12} h^2\partial_z w\partial_x \hat{u} - \frac{1}{12} h^2\partial_z(\hat{u}\partial_x w) - \frac{1}{12} h^2 w\partial_{zz} w - \frac{1}{12} h^2\partial_{zz} p.$$

4

To summarize, we get:

$$\begin{cases} \partial_t\left(h\overline{u}\right) + \partial_x\left(h\overline{u}^2 + \frac{1}{2}gh^2 + h\overline{p}\right) + \partial_x\left(h\overline{\hat{u}^2}\right) = \left(gh + p_b\right)\partial_x H, \\[2mm] \partial_t\left(h\overline{w}\right) + \partial_x\left(h\overline{u}\,\overline{w}\right) + \partial_x\left(h\overline{\hat{u}\hat{w}}\right) = p_b \\[2mm] \partial_t\left(h\xi\right) + \partial_x\left(\overline{u}h\xi\right) = \frac{1}{12}h^2\partial_z w\partial_x\hat{u} - \frac{1}{12}h^2\partial_z(\hat{u}\partial_x w) - \frac{1}{12}h^2 w\partial_{zz}w - \frac{1}{12}h^2\partial_{zz}p. \end{cases}$$

To close the system, as mentioned before, we shall make some assumptions on the given vertical profiles of the unknowns of the problem. We will suppose that deviations of the horizontal velocity u are small. This will allow us to neglect the deviation from its vertical average. We shall suppose as well some information on the second-order derivatives. More explicitly, we shall assume that w has a linear vertical profile and the non-hydrostatic pressure p has a quadratic vertical profile:

$$u(\cdot, z) \in \mathbb{P}_0,\ w(\cdot, z) \in \mathbb{P}_1,\ p(\cdot, z) \in \mathbb{P}_2.$$

Note that the hypothesis of constant vertical profile for the horizontal velocity corresponds to a shallow water regime. In fact, if we take $p = 0$ in (4), we would get the SWE.

From (1a), using the assumption $w(\cdot, z) \in \mathbb{P}_1$ and $u(\cdot, z) \in \mathbb{P}_0$, one gets

$$w = w_b + \partial_z w(z + H) = w_b - \partial_x\overline{u}(z + H),$$

where $w_b = w|_{z=-H}$ is the vertical velocity at the bottom. Now, using this fact, from the definition of $\overline{w}$ and (3) respectively one gets

$$\overline{w} = w_b - \frac{1}{2}h\partial_x\overline{u}, \qquad w_b = -\overline{u}\partial_x H - \partial_t H. \tag{8}$$

The fact that $p(\cdot, z) \in \mathbb{P}_2$ means that $\partial_{zz}p$ does not depend on z. Moreover, the non-hydrostatic pressure at the surface vanishes. Therefore, using for instance the trapezoidal quadrature rule, one gets

$$\overline{p} = \frac{1}{2}p_b - \frac{1}{12}h^2\partial_{zz}p,$$

where $p_b = p|_{z=-H}$ corresponds to the non-hydrostatic pressure at the bottom.

Remark 1. *One could also consider a linear vertical profile for the non-hydrostatic pressure. In that case, the relation*

$$\overline{p} = \frac{1}{2}p_b$$

holds, and we get the system introduced in [13].

To sum up, collecting all the equations described before, and skipping the notation in bars to denote depth-averaged variables, the system reads as:

$$\partial_t h + \partial_x\left(hu\right) = 0, \tag{9a}$$

$$\partial_t\left(hu\right) + \partial_x\left(uhu + \frac{1}{2}gh^2 + hp\right) = \left(gh + p_b\right)\partial_x H, \tag{9b}$$

$$\partial_t\left(hw\right) + \partial_x\left(uhw\right) = p_b, \tag{9c}$$

$$\partial_t\left(h\xi\right) + \partial_x\left(uh\xi\right) = p - \frac{1}{2}p_b, \tag{9d}$$

$$w = w_b - \frac{1}{2}h\partial_x u, \qquad w_b = -u\partial_x H - \partial_t H, \tag{9e}$$

$$\xi = -\beta h\partial_x u. \tag{9f}$$

where β is a free parameter. In the previous deduction it was given by $\beta = 1/12$ for the case $p \in \mathbb{P}_2$, and $\beta = 0$ for the assumption $p \in \mathbb{P}_1$. Remark that here and in the rest of the paper we are choosing $u(\cdot, z) \in \mathbb{P}_0$, $w(\cdot, z) \in \mathbb{P}_1$. Nevertheless it could be chosen otherwise.

Proposition 1. *Smooth solutions for system (9) satisfies the following entropy equality:*

$$\partial_t \left(h \left(\frac{u^2}{2} + \frac{w^2}{2} + \frac{\xi^2}{2\beta} + g \left(\frac{h}{2} - H \right) \right) \right) + \partial_x \left(hu \left(\frac{u^2}{2} + \frac{w^2}{2} + \frac{\xi^2}{2\beta} + p + g\eta \right) \right) = -(gh + p_b)\partial_t H \tag{10}$$

Proof. The proof is done as it is usual in this kind of models. First, using (9a), we rewrite (9b), (9c) and (9d) as

$$h\partial_t u + hu\partial_x u + \partial_x (hp) = p_b \partial_x H - gh\partial_x \eta,$$

$$h\partial_t w + hu\partial_x w = p_b,$$

$$h\beta^{-1}\partial_t \xi + hu\beta^{-1}\partial_x \xi = \beta^{-1} \left(p - \frac{1}{2}p_b \right)$$

Now multiply these equations by u, w, and ξ respectively and combine them with (9a) to obtain:

$$\partial_t \left(h\frac{u^2}{2} \right) + \partial_x \left(hu \left(\frac{u^2}{2} + p + g\eta \right) \right) = g\eta \partial_x (hu) + hp\partial_x u + p_b u \partial_x H,$$

$$\partial_t \left(h\frac{w^2}{2} \right) + \partial_x \left(hu\frac{w^2}{2} \right) = wp_b,$$

$$\partial_t \left(h\frac{\xi^2}{2\beta} \right) + \partial_x \left(hu\frac{\xi^2}{2\beta} \right) = \frac{1}{\beta}\xi \left(p - \frac{1}{2}p_b \right)$$

Adding these three equations one obtains:

$$\partial_t \left(h \left(\frac{u^2}{2} + \frac{w^2}{2} + \frac{\xi^2}{2\beta} \right) \right) + \partial_x \left(hu \left(\frac{u^2}{2} + \frac{w^2}{2} + \frac{\xi^2}{2\beta} + p + g\eta \right) \right) = g\eta\partial_x(hu) + p \left(h\partial_x u + \frac{\xi}{\beta} \right) + p_b \left(u\partial_x H + w - \frac{\xi}{2\beta} \right)$$

Now, remark that from (9e) one may write

$$u\partial_x H + w - \frac{\xi}{2\beta} = -\partial_t H - \frac{1}{2} \left(h\partial_x u + \frac{\xi}{\beta} \right).$$

We also rewrite

$$\eta\partial_x(hu) = -\eta\partial_t h = -\partial_t \left(h \left(\frac{h}{2} - H \right) \right) - h\partial_t H.$$

Then, using the definition of ξ by (9f), the result follows. □

3. Rewriting of classical Boussinesq and non-hydrostatic pressure systems

In this Section, we intend to show that (9) gives us a general framework that recovers many of the classical known models for dispersive and non-hydrostatic fluids.

To do so, let us describe some of the well-known systems used for dispersive water waves. In particular we focus on the models described in [13], [14], [3], [6], [4] which shall be denoted respectively by (BMSS), (YKC), (GN), (PER), (MS). For each of them we describe the process of recasting these systems into the form of (9):

- Non-hydrostatic pressure system derived by Bristeau et al. in [13].

  This system can be written in the general formulation (9) by setting $\beta = 0$. In this case, given that $\xi = -\beta h\partial_x u = 0$, we get

$$p = \frac{1}{2}p_b, \tag{11}$$

6

and therefore the equations (9d) and (9f) can be suppressed resulting in:

$$
\begin{cases}
\partial_t h + \partial_x (hu) = 0, \\[2mm]
\partial_t (hu) + \partial_x \left(hu^2 + \dfrac{1}{2} gh^2 + hp \right) = (gh + 2p)\, \partial_x H, \\[2mm]
\partial_t (hw) + \partial_x (huw) = 2p, \\[2mm]
w = w_b - \dfrac{1}{2} h\partial_x u, \qquad w_b = -u\partial_x H - \partial_t H.
\end{cases}
\tag{BMSS}
$$

- Non-hydrostatic pressure system derived by Yamazaki et al. in [14].

  We set again $\beta = 0$. Then, in a similar way as before, this system can be written in the general formulation (9) by neglecting the convective terms in the momentum equation for the variable w :

$$
\begin{cases}
\partial_t h + \partial_x (hu) = 0, \\[2mm]
\partial_t (hu) + \partial_x \left(hu^2 + \dfrac{1}{2} gh^2 + hp \right) = (gh + 2p)\, \partial_x H, \\[2mm]
\partial_t (hw) = 2p, \\[2mm]
w = w_b - \dfrac{1}{2} h\partial_x u, \qquad w_b = -u\partial_x H - \partial_t H.
\end{cases}
\tag{YKC}
$$

Remark 2. *The formulation used here for (YKC) differs from the one introduced in [14]. In [14] the conserved variables are not used and the system is written in terms of the pressure at the bottom p_b rather than the average pressure p, where (11) is assumed. Moreover, [14] makes an extra hypothesis and simplifies the third equation to*

$$
h\partial_t w = 2p,
$$

by assuming that $h \approx H$. We shall not make this assumption here and we shall use the formulation (YKC).

- Green-Naghdi system derived in [3].

  The system written as in [15], [19] or [20], reads:

$$
\begin{cases}
\partial_t h + \partial_x (hu) = 0, \\[2mm]
\partial_t (hu) + \partial_x \left(hu^2 + \dfrac{1}{2} gh^2 + h^2 \left(\dfrac{\mathcal{P}}{3} + \dfrac{Q}{2} \right) \right) = \left(gh + h \left(\dfrac{\mathcal{P}}{2} + Q \right) \right) \partial_x H, \\[2mm]
\mathcal{P} = -h \left(\partial_{tx} u + u\partial_{xx} u - (\partial_x u)^2 \right), \\[2mm]
Q = \partial_x z_b (\partial_t u + u\partial_x u) + u^2 \partial_{xx} z_b.
\end{cases}
\tag{GN}
$$

This system was written in an equivalent form as a non-hydrostatic pressure shallow water system in [15]. The general formulation (9) described in this work recovers the Green-Naghdi system by setting $\beta = 1/12$.

It is interesting to remark that in the particular case of flat bottom, as stated in [13], the system is equivalent to

$$\begin{cases} \partial_t h + \partial_x (hu) = 0, \\[2mm] \partial_t (hu) + \partial_x \left(hu^2 + \frac{1}{2} gh^2 + hp \right) = 0, \\[2mm] \partial_t (hw) + \partial_x (huw) = \frac{3}{2} p, \\[2mm] w = -\frac{1}{2} h \partial_x u. \end{cases} \qquad (12)$$

Indeed from $\partial_x H = 0$, and equations (9e)-(9f) we get

$$w = -\frac{1}{2} h \partial_x u, \text{ and } \xi = -\frac{1}{12} h \partial_x u,$$

therefore

$$w = 6\xi. \qquad (13)$$

Using the equations in (9c)-(9d), and (13), it can be easily deduced that

$$p_b = \frac{3}{2} p. \qquad (14)$$

So that the general formulation (9) is reduced to (12) in this situation. This means that, for the case of flat bottom, this system is the same as (BMSS) but setting $p_b = \frac{3}{2} p$. A particular analysis under this hypothesis of flat bottom, as well as an efficient numerical strategy to solve it was proposed in [13] and [18] respectively.

- Classical system derived by Peregrine in [6]. This system was introduced in the form:

$$\begin{cases} \partial_t h + \partial_x (hu) = 0, \\[2mm] \partial_t (hu) + \partial_x \left(hu^2 + \frac{1}{2} gh^2 \right) = gh \partial_x H + \frac{1}{2} H^2 \partial_{xxt} (Hu) - \frac{1}{6} H^3 \partial_{xxt} u. \end{cases} \qquad \text{(PER)}$$

Note that the momentum equation in (PER) can be written equivalently as

$$\partial_t (hu) + \partial_x \left(hu^2 + \frac{1}{2} gh^2 + H (p_1 + p_2) \right) = (gh + 2p_1 + 3p_2) \, \partial_x H,$$

where

$$p_1 = \partial_t (Hw_1), \qquad w_1 = -\frac{1}{2} u \partial_x H - \frac{1}{2} H \partial_x u,$$

$$p_2 = \partial_t (Hw_2), \qquad w_2 = \frac{1}{6} H \partial_x u.$$

Let us define

$$p = p_1 + p_2, \qquad p_b = 2p_1 + 3p_2,$$

$$w = 2w_1 + 3w_2, \qquad \xi = w_1 + w_2 - \frac{1}{2} w.$$

Then, system (PER) may also be written using the formulation (9). This can be done by neglecting convective terms in the momentum equations (9c)-(9d), assuming $\partial_t H = 0$, and using the assumption $h \approx H$ in equa-

tions (9c)-(9f) and in the term $\partial_x(hp)$ of equation (9b):

$$\begin{cases} \partial_t h + \partial_x (hu) = 0, \\[2mm] \partial_t (hu) + \partial_x \left(hu^2 + \frac{1}{2} gh^2 + Hp \right) = (gh + p_b) \partial_x H, \\[2mm] \partial_t (Hw) = p_b, \\[2mm] \partial_t (H\xi) = p - \frac{1}{2} p_b, \\[2mm] w = w_b - \frac{1}{2} H\partial_x u, \qquad w_b = -u\partial_x H, \\[2mm] \xi = -\frac{1}{12} H\partial_x u. \end{cases} \tag{15}$$

Remark that the assumption $h \approx H$ is usually made in the derivations of this type of models and in particular in the deduction proposed in [6].

- Madsen-Sørensen system derived in [4].

  In [4], the authors propose a novel Boussinesq-type system with enhanced dispersive properties. The derivation is done by taking as a starting point the Peregrine equations and introducing a free parameter B that is then optimized to improve the dispersive relations obtained. The genuine system derived in [4], reads

$$\begin{cases} \partial_t h + \partial_x (hu) = 0, \\[2mm] \partial_t (hu) + \partial_x \left(hu^2 + \frac{1}{2} gh^2 \right) = gh\partial_x H + \frac{1}{2} H^2 \partial_{xxt} (Hu) - \frac{1}{6} H^3 \partial_{xxt} u + B\psi, \end{cases} \tag{MS}$$

where ψ is given by

$$\psi = H^2 \partial_{xxt} (Hu) + gH^3 \partial_{xxx} \eta + 2gH^2 \partial_{xx} \eta \partial_x H. \tag{16}$$

In [4], a dispersion analysis of the linearised system is done, similar to the one performed in this paper in Subsection 4.2. In [4] authors found the values of $B = 1/15$ and $B = 1/21$ to be optimal to match with the Stokes linear theory. These values will be adopted as well in this paper.

First, note that following the same ideas as for Peregrine's system, one can rewrite the equations (MS) in a similar way as (15):

$$\begin{cases} \partial_t h + \partial_x (hu) = 0, \\[2mm] \partial_t (hu) + \partial_x \left(hu^2 + \frac{1}{2} gh^2 + Hp \right) = (gh + p_b) \partial_x H + B\psi, \\[2mm] \partial_t (Hw) = p_b, \\[2mm] \partial_t (H\xi) = p - \frac{1}{2} p_b, \\[2mm] w = w_b - \frac{1}{2} H\partial_x u, \qquad w_b = -u\partial_x H, \\[2mm] \xi = -\frac{1}{12} H\partial_x u. \end{cases} \tag{17}$$

The term ψ contains high-order derivatives which we would like to avoid. To do so, using again similar manipulations as before, one may write

$$\psi = \partial_x \left(H^2 \partial_{xt} (Hu) + gH^3 \partial_{xx} \eta \right) - \left(2H\partial_{xt} (Hu) + gH^2 \partial_{xx} \eta \right) \partial_x H.$$

9

Now, define the new variables $\widetilde{p}$, $\widetilde{p}_b$, and $\widetilde{w}$ by

$$\widetilde{p} = p - BH\partial_{xt}(Hu) - BgH^2\partial_{xx}\eta,$$

$$\widetilde{p}_b = p_b - 2BH\partial_{xt}(Hu) - BgH^2\partial_{xx}\eta,$$

$$\widetilde{w} = w - 2B\partial_x(Hu).$$

Then, system (17) may be written as

$$\begin{cases} \partial_t h + \partial_x(hu) = 0, \\[2mm] \partial_t(hu) + \partial_x\left(hu^2 + \dfrac{1}{2}gh^2 + H\widetilde{p}\right) = (gh + \widetilde{p}_b)\,\partial_x H, \\[2mm] \partial_t(H\widetilde{w}) = \widetilde{p}_b + BgH^2\partial_{xx}\eta, \\[2mm] \partial_t(H\xi) = \widetilde{p} - \dfrac{1}{2}\widetilde{p}_b + \dfrac{1}{2}BgH^2\partial_{xx}\eta, \\[2mm] \widetilde{w} = (1 + 2B)\,w_b - \dfrac{1}{2}(4B + 1)\,H\partial_x u, \qquad w_b = -u\partial_x H, \\[2mm] \xi = -\dfrac{1}{12}H\partial_x u. \end{cases} \qquad (18)$$

Therefore, the system derived in [4] can also be recast into a non-hydrostatic formulation. Nevertheless, opposed to the previous cases, we still have here a second-order derivative for the term $\partial_{xx}\eta$. In the next subsection, we intend to give a more general formulation that collects all of the studied cases and includes only first-order derivatives. Remark that this is done so that one could recover systems similar to the Madsen-Sørensen. Nevertheless, if one is interested just in the previous cases ($B = 0$), then (9) suffices.

3.1. A general formulation

Given what has been said before, we aim now to propose a general formulation for commonly used dispersive systems that extends (9). The system shall be written using only first-order derivatives of the variables. To do so, let us consider first the following extension of (9):

$$\partial_t h + \partial_x(hu) = 0, \qquad\qquad\qquad\qquad\qquad\qquad\qquad (19a)$$

$$\partial_t(hu) + \partial_x\left(uhu + \dfrac{1}{2}gh^2 + hp\right) = (gh + 2(p - q))\,\partial_x H, \qquad (19b)$$

$$\partial_t(hw) + \partial_x(uhw) = 2(p - q) + Bgh^2\partial_{xx}\eta, \qquad\qquad\quad (19c)$$

$$\partial_t(h\xi) + \partial_x(uh\xi) = q + \dfrac{1}{2}Bgh^2\partial_{xx}\eta, \qquad\qquad\qquad\quad (19d)$$

$$w = (1 + 2B)\,w_b - \dfrac{1}{2}(4B + 1)\,h\partial_x u, \quad w_b = -u\partial_x H - \partial_t H, \quad (19e)$$

$$\xi = -\beta h\partial_x u. \qquad\qquad\qquad\qquad\qquad\qquad\qquad\qquad (19f)$$

Note that setting $B = 0$ and $q = p - \dfrac{1}{2}p_b$ in (19) one recovers (9). Nevertheless, for $B \neq 0$, (19) includes second-order derivatives of the free-surface that originally appears in (18) and we would like to avoid. To do so, let us define

$$\zeta = B\partial_x\eta.$$

First remark that, from (19a), one has

$$\partial_t(h\zeta) = -B\partial_x(hu)\,\partial_x\eta - Bh\partial_{xx}(hu) - Bh\partial_{tx}H = -\zeta\partial_x(hu) - Bh\partial_{tx}H - Bh\partial_{xx}(hu). \qquad (20)$$

10

Note that the last term, $Bh\partial_{xx}(hu)$, can be written as

$$Bh\partial_{xx}(hu) = B\left(hu\partial_{xx}h + 2h\partial_x h\partial_x u + h^2\partial_{xx}u\right) = Bhu\partial_{xx}h + B\partial_x\left(h^2\partial_x u\right),$$

and using equation (19f)

$$Bhu\partial_{xx}h + B\partial_x\left(h^2\partial_x u\right) = Bhu\partial_{xx}\eta + Bhu\partial_{xx}H - B\beta^{-1}\partial_x(h\xi) = hu\partial_x\zeta + Bhu\partial_{xx}H - B\beta^{-1}\partial_x(h\xi).$$

Thus, equation (20) yields

$$\partial_t(h\zeta) + \partial_x\left(uh\zeta - B\beta^{-1}h\xi\right) = -Bhu\partial_{xx}H - Bh\partial_{tx}H. \tag{21}$$

In the following we will assume $\partial_{xx}H \approx 0$ and $\partial_{tx}H \approx 0$. These assumptions are in agreement with the mild bottom variation hypothesis made in [4]. In any case, these terms may be retained and the resulting system may be also recast into the general formulation as it is shown in Remark 3.

Now, using the fact that

$$Bgh^2\partial_{xx}\eta = gh^2\partial_x\zeta = g\left(\partial_x\left(h^2\zeta\right) - 2h\zeta\partial_x h\right),$$

system (19) may be written as

$$\partial_t h + \partial_x(hu) = 0, \tag{22a}$$

$$\partial_t(hu) + \partial_x\left(uhu + \frac{1}{2}gh^2 + hp\right) = (gh + 2(p-q))\partial_x H, \tag{22b}$$

$$\partial_t(hw) + \partial_x\left(uhw - gh^2\zeta\right) + 2gh\zeta\partial_x h = 2(p-q), \tag{22c}$$

$$\partial_t(h\xi) + \partial_x\left(uh\xi - \frac{1}{2}gh^2\zeta\right) + gh\zeta\partial_x h = q, \tag{22d}$$

$$w = (1+2B)w_b - \frac{1}{2}(4B+1)h\partial_x u, \quad w_b = -u\partial_x H - \partial_t H, \tag{22e}$$

$$\xi = -\beta h\partial_x u. \tag{22f}$$

$$\partial_t(h\zeta) + \partial_x\left(uh\zeta - B\beta^{-1}h\xi\right) = 0, \tag{22g}$$

where the coefficient $B\beta^{-1}$ is set to zero when $\beta = 0$. Remark that setting $B = 0$, $\zeta = 0$ and $q = p - \frac{1}{2}p_b$ we recover (9).

System (22) has now the advantage that it only includes first-order derivatives and covers all the well-known and leading dispersive systems that are used in ocean engineering.

Remark that in some cases additional hypothesis should be done. Some terms are neglected in the derivation of some classical dispersive models, whereas they are present in this general formulation. More explicitly, we have seen in Section 3 that the system (BMSS) proposed in [13] is recovered by setting $B = \beta = 0$. System (GN) introduced in [3] falls directly into the general formulation for $B = 0$, $\beta = 1/12$. The system (YKC) found in [14] may be recovered by setting $B = \beta = 0$ and neglecting the convective terms $\partial_x(hw)$ and $\partial_x(h\xi)$. In a similar way the system (PER) derived in [6] can be recovered by setting $B = 0$, $\beta = 1/12$, neglecting the convective terms $\partial_x(hw)$, $\partial_x(h\xi)$, and replacing h by H in equations (22c)-(22g) as well as in the term $\partial_x(hp)$ in equation (22b). Remark that these assumptions were already made in [6] in the derivation of the model. Finally, (MS) introduced in [4] may be written in the form (22) using the similar hypothesis as for (PER) and using $B = 1/21$ or $B = 1/15$. All of this is summarized in Table 1. Moreover, one may not use these additional assumptions which would leads us, depending on the values of B and β in (22), to a system that provides a new generalization to the well-known dispersive systems (PER), (YKC) and (MS). The difference being that all the terms that were neglected during their original derivation are now included. This means that, for $B = 0$ and $\beta = 0$ we obtain (BMSS), which is an extension of the original (YKC); for $B = 0$ and $\beta = 1/12$ we obtain (GN) which may be seen as an extension of the original (PER); and for B free parameter and $\beta = 1/12$ we obtain an extension of the original (MS) which shall be denoted by (EMS) in what follows.

	Coefficients and assumptions		
	B	β	Assumptions
BMSS	0	0	×
YKC	0	0	$\partial_x(uhw) = \partial_x(uh\xi) \approx 0,\ \partial_t(hw) \approx h\partial_t w$
GN	0	$\frac{1}{12}$	×
PER	0	$\frac{1}{12}$	$\partial_x(uhw) = \partial_x(uh\xi) \approx 0,\ h \approx H$
MS	$\frac{1}{15},\ \frac{1}{21}$	$\frac{1}{12}$	$\partial_x(uhw) = \partial_x(uh\xi) \approx 0,\ h \approx H$

Table 1: Choice of parameters and additional assumptions needed in order to recover classical dispersive models from (22).

Furthermore, we will see in Section 4.2 that this new generalization of the classical dispersive systems will not change the linear dispersion relations satisfied by its original counterpart.

Remark 3. *Concerning the terms that were neglected in equation* (21)*,*

$$Bhu\partial_{xx}H + Bh\partial_{tx}H,$$

note that, they can be also rewritten as

$$\partial_t(Bh\partial_x H) + \partial_x(Bhu\partial_x H).$$

Then equation (21) *reads*

$$\partial_t(h(\zeta + B\partial_x H)) + \partial_x\left(uh(\zeta + B\partial_x H) - B\beta^{-1}h\xi\right) = 0.$$

Therefore, one can define $\tilde{\zeta} = \zeta + B\partial_x H$ *and equations* (22c)*,* (22d) *and* (22g) *read as*

$$\partial_t(hw) + \partial_x\left(uhw - gh^2\tilde{\zeta}\right) + 2gh\tilde{\zeta}\partial_x h = 2(p-q) - gBh^2\partial_{xx}H,$$

$$\partial_t(h\xi) + \partial_x\left(uh\xi - \frac{1}{2}gh^2\tilde{\zeta}\right) + gh\tilde{\zeta}\partial_x h = 2(p-q) - \frac{1}{2}gBh^2\partial_{xx}H,$$

$$\partial_t\left(h\tilde{\zeta}\right) + \partial_x\left(uh\tilde{\zeta} - B\beta^{-1}h\xi\right) = 0.$$

The resulting system is then first-order, except for the term $\partial_{xx}H$*. Nevertheless, this term may be considered as data and should not give major difficulties. Another possibility is to neglect it as it is done in [4].*

Remark 4. *In Section 4, the system* (22) *will be relaxed and approximated by a hyperbolic system. To do so, we remark that from* (22) *one may deduce some relations that will be of interest in the relaxation process. More explicitly, in the case of a flat bottom one gets*

$$w = -\mu h\partial_x u, \qquad \xi = -\beta h\partial_x u, \qquad \mu = \frac{1}{2}(4B+1),$$

and therefore

$$\mu\xi = \beta w.$$

In a similar way, we can deduce that for a flat bottom one gets

$$2\beta p = (\mu + 2\beta)q + \frac{1}{2}(\mu - 2\beta)gh^2\partial_x\zeta.$$

12

For the sake of completeness, let us show how to obtain the last equation:

Multiplying equation (22c) *by* β :

$$\beta\left(\partial_t(hw) + \partial_x(uhw)\right) = \beta g h^2 \partial_x \zeta + 2\beta(p - q).$$

Now, using that for a flat bottom $\mu\xi = \beta w$, *the above relation becomes:*

$$\mu\left(\partial_t(h\xi) + \partial_x(uh\xi)\right) = \beta g h^2 \partial_x \zeta + 2\beta(p - q).$$

Now, using equation (22d) *multiplied by* μ *one has:*

$$\mu\left(\partial_t(h\xi) + \partial_x(uh\xi)\right) = \frac{1}{2}\beta g h^2 \partial_x \zeta + \mu q,$$

and the result follows.

Remark 5. *The classical Boussinesq-type systems* (YKC)*,* (GN)*,* (PER) *or* (MS) *were derived under the assumption of stationary bed, that is,* $\partial_t H = 0$. *This general formulation* (22) *allows us to easily extend them for the case of non-stationary bottoms. This can be done by using the sea-bed boundary condition* (3)

$$w_b = -u\partial_x H - \partial_t H.$$

3.2. Modeling of breaking waves

As pointed out in [17], [18], [21] among others, in shallow water flow complex events can be observed related to turbulent processes. One of these processes corresponds to the breaking of waves near the coast. As it will be seen in the numerical tests shown in the next section, the PDE systems considered in this paper cannot describe this process without an additional term that allows the model to dissipate the required amount of energy in such situations. In this work, we adopt a simplified version of the breaking mechanism introduced in [17], [22] and later adopted for approximated hyperbolic dispersive systems in [18] where a friction term is added to the right hand side of the equations:

$$\partial_t(hw) + \partial_x\left(uhw - gh^2\zeta\right) + 2gh\zeta\partial_x h = 2(p - q) + \kappa w, \qquad \kappa = -2b|\partial_x(hu)|,$$

$$\partial_t(h\xi) + \partial_x\left(uh\xi - \frac{1}{2}gh^2\zeta\right) + gh\zeta\partial_x h = q + \kappa\xi.$$

Note that, as it was pointed out in Remark 4, in the case of flat bottom we have $\mu\xi = \beta w$ and the amount of energy dissipated is consistent in both equations.

The breaking mechanism must be combined with a breaking criteria to switch on and off this extra dissipation term, and this is controlled by the parameter b. The definition of this empirical parameter b is based on a quasi-heuristic strategy to determine when the breaking occurs (see [17], [21] and references therein). In this work it is given by

$$b = 1 - \frac{\partial_x(hu)}{U_1},$$

where wave energy dissipation associated with breaking begins when $|\partial_x(hu)| \geq U_1$ and continues as long as $|\partial_x(hu)| \geq U_2$, where

$$U_1 = b_1\sqrt{gh}, \qquad U_2 = b_2\sqrt{gh},$$

denote the flow speeds at the onset and termination of the wave-breaking process. b_1, b_2 are coefficients that should be calibrated through laboratory experiments. In this work, as in [17], [18] or [21], we use $b_1 = 0.5$ and $b_2 = 0.15$ for all the test cases studied.

4. A hyperbolic approximation

The general formulation (22) has two main advantages. On the one hand, as it has already been said, it covers all the classical and well known dispersive systems. Moreover, it allows us to propose a generalization of some of these systems by including the terms that were neglected in their original derivation. On the other hand, (22) corresponds to a first-order PDE system instead of a higher-order PDE.

This will allow us to propose a general, simple and efficient algorithm to solve it numerically, based on ideas presented in [17]. Let us remark that, even though (9) or (22) only presents first-order derivatives, we have merely rewritten in a different way the original systems and they are in fact equivalent. This means that the original nature of the systems has not changed. See for instance how the numerical strategy used in [17] requires to solve implicitly the pressure, as one usually does in parabolic equations, in order to avoid the restrictive time step that an explicit scheme would need.

However, implicit numerical schemes for this class of PDE systems will lead to solving linear systems at each time step of the numerical algorithm, which will become the main bottleneck of the algorithm from a computational time point of view. Moreover, the complexity of the numerical scheme, the numerical stencil and the condition number of the underlying linear system to be solved will increase with the order of the scheme. This makes high-order schemes for Boussinesq-type systems not so efficient as one would prefer. The aforementioned problems are even more difficult to be dealt with for the case of high-order PDE systems such as (MS).

Additional challenges come up when designing robust and efficient numerical schemes in the context of dispersive shallow flows. For example, the presence of wetting and drying fronts and the ability of the numerical scheme to preserve the positivity of the total water depth is not an easy task. Another important property is related to well-balancing: we expect the scheme to preserve stationary solutions such as lake-at-rest steady states. Moreover, the selection of a good linear solver plays an important role in the computational efficiency of the final scheme.

The aim is then to deduce a hyperbolic system that may be seen as a relaxation of the system (22), which can be efficiently solved by arbitrary high-order numerical methods. To do so, we consider the following modified system:

$$\partial_t h + \partial_x (hu) = 0, \tag{23a}$$

$$\partial_t (hu) + \partial_x \left(uhu + \frac{1}{2} gh^2 + hp \right) = (gh + 2(p - q)) \partial_x H - \tau_b, \tag{23b}$$

$$\partial_t (hw) + \partial_x \left(uhw - gh^2 \zeta \right) + 2gh\zeta \partial_x h = 2(p - q) + \kappa w, \tag{23c}$$

$$\partial_t (h\xi) + \partial_x \left(uh\xi - \frac{1}{2} gh^2 \zeta \right) + gh\zeta \partial_x h = q + \kappa \xi, \tag{23d}$$

$$\partial_t (hp) + \partial_x (uhp) + \gamma_1 c^2 (w - \mu_B w_b + \mu h \partial_x u) = 0, \qquad w_b = -u\partial_x H - \partial_t H \tag{23e}$$

$$\partial_t (hq) + \partial_x (uhq) + \gamma_2 c^2 (\xi + \beta h \partial_x u) = 0, \tag{23f}$$

$$\partial_t (h\zeta) + \partial_x \left(uh\zeta - B\beta^{-1} h\xi \right) = 0, \tag{23g}$$

where $\mu = (4B + 1)/2$, $\mu_B = 2B + 1$ and β, B are free parameters. $c = \alpha \sqrt{gH_0}$ is a given constant celerity, H_0 being a typical average still water depth and $\alpha > 1$. γ_1 and γ_2 are two parameters to be chosen conveniently.

The approximation is based on a modified system in which the divergence constraint on the velocity field is coupled with the other conservation laws, following the ideas of the so-called hyperbolic divergence cleaning. This hyperbolic divergence cleaning was applied in the context of the generalized Lagrangian multiplier (GLM) method for the magnetohydrodynamics equations put forward in [23], [24]. We suggest a formulation in which the divergence errors are transported with a finite speed of c. Remark that, when $\alpha \to +\infty$, the system (23) formally converges to (22). We refer the reader to [18] where a similar approach was proposed for the system (BMSS) and (12). In the subsequent Section, we study the hyperbolicity of the augmented system.

Finally, the bottom friction is included in the model via a usual Manning-type friction formula [25] for the bottom

shear stress τ_b that reads

$$\tau_b = n_m^2 ghu \frac{|u|}{h^{4/3}}.$$

Remark 6. *We want to ensure that the new system satisfies a similar relation between the variables w, ξ and p, p_b for the case of flat bottom, as it was stated in Remark 4. This can be obtained by choosing*

$$\gamma_1 = \mu + 2\beta, \quad \gamma_2 = 2\mu,$$

and hereinafter we will set γ_1 and γ_2 as described above.

4.1. Eigenstructure of the modified equations

System (23) can be written in compact matrix-vector form as

$$\partial_t \mathbf{U} + \partial_x \mathbf{F}(\mathbf{U}) + \mathbf{B}(\mathbf{U})\partial_x \mathbf{U} = \mathbf{S}(\mathbf{U}), \tag{24}$$

with

$$\mathbf{U} = \begin{pmatrix} h \\ hu \\ hw \\ h\xi \\ hp \\ hq \\ h\zeta \end{pmatrix}, \; \mathbf{F}(\mathbf{U}) = \begin{pmatrix} hu \\ uhu + hp \\ uhw - gh^2\zeta \\ uh\xi - \frac{1}{2}gh^2\zeta \\ hu\left(p + \gamma_1\mu c^2\right) \\ hu\left(q + \gamma_2\beta c^2\right) \\ uh\zeta - B\beta^{-1}h\xi \end{pmatrix}, \; \mathbf{S}(\mathbf{U}) = \begin{pmatrix} 0 \\ -\tau_b \\ 2(p - q) + \kappa w \\ q + \kappa\xi \\ -\gamma_1 c^2(w + \mu_B\partial_t H) \\ -\gamma_2 c^2\xi \\ 0 \end{pmatrix}, \; \mathbf{B}(\mathbf{U})\partial_x \mathbf{U} = \begin{pmatrix} 0 \\ (gh + 2(p - q))\partial_x\eta - 2(p - q)\partial_x h \\ 2gh\zeta\partial_x h \\ gh\zeta\partial_x h \\ \gamma_1 c^2 u\partial_x\left(\frac{1}{2}h - \mu_B\eta\right) \\ -\gamma_2\beta c^2 u\partial_x h \\ 0 \end{pmatrix}.$$

Equivalently, the system may also be written in quasi-linear form:

$$\partial_t \mathbf{U} + \mathbf{A}(\mathbf{U})\partial_x \mathbf{U} = \mathbf{S}(\mathbf{U}),$$

with

$$\mathbf{A}(\mathbf{U}) = \mathbf{J_F}(\mathbf{U}) + \mathbf{B}(\mathbf{U}),$$

where $\mathbf{J_F} = \partial\mathbf{F}/\partial\mathbf{U}$ is the Jacobian of the flux $\mathbf{F}$ with respect to the conserved variables $\mathbf{U}$. Some easy calculations show that the eigenvalues of the matrix $\mathbf{A}(\mathbf{U})$ are

$$\lambda_{1,2,3} = u, \quad \lambda_{4,5} = u \pm \sqrt{B\beta^{-1}gh/2}, \quad \lambda_{6,7} = u \pm \sqrt{gh + p + \gamma_1\mu c^2}.$$

Therefore, system (23) is hyperbolic provided that $B\beta^{-1}gh/2 \geq 0$ and $gh + p + \gamma_1\mu c^2 \geq 0$. This means that (23) may be solved by means of the usual numerical schemes for non-conservative hyperbolic systems, provided that α is sufficiently large.

Remark 7. *Note that the usual hydrostatic solutions corresponding to the non-linear shallow water equations can be recovered by setting $B = 0$ and imposing the initial conditions*

$$p(x, 0) = q(x, 0) = \zeta(x, 0) = 0.$$

15

4.2. Linear dispersion relation

As it was stated previously, system (23) intends to be a generalization of classical well-known dispersive systems. Therefore, the dispersive relations satisfied by this new system should be studied. To do so we consider the approach that is usually followed (see [4], [18], [26], [27], [28]). More explicitly, the case of flat bottom is considered and system (23) is linearised around the steady state solution $h = H$, $u = 0$, $w = 0$, $\xi = 0$, $p = 0$, $q = 0$, $\zeta = 0$. An asymptotic expansion in the form

$$f = f^{(0)} + \epsilon f^{(1)} + O(\epsilon^2),$$

is considered, where f stands for any generic variable of the system. After some easy calculations and neglecting $O(\epsilon^2)$ terms, the following linearised system is obtained:

$$
\begin{cases}
\partial_t \eta^{(1)} + H \partial_x u^{(1)} = 0, \\[2mm]
\partial_t u^{(1)} + g \partial_x \eta^{(1)} + \partial_x p^{(1)} = 0, \\[2mm]
H \partial_t w^{(1)} - 2 \left(p^{(1)} - q^{(1)} \right) - gH^2 \partial_x \zeta^{(1)} = 0, \\[2mm]
H \partial_t \xi^{(1)} - q^{(1)} - \dfrac{1}{2} gH^2 \partial_x \zeta^{(1)} = 0, \\[2mm]
H \partial_t p^{(1)} + \gamma_1 c^2 \mu H \partial_x u^{(1)} + \gamma_1 c^2 w^{(1)} = 0, \\[2mm]
H \partial_t q^{(1)} + \gamma_2 c^2 \beta H \partial_x u^{(1)} + \gamma_2 c^2 \xi^{(1)} = 0, \\[2mm]
H \partial_t \zeta^{(1)} - B\beta^{-1} H \partial_x \xi^{(1)} = 0.
\end{cases}
\tag{25}
$$

We shall now proceed to perform a Stokes-type Fourier analysis and look for solutions of the form,

$$f^{(1)}(x, t) = f_0 e^{i(\omega t - kx)}, \tag{26}$$

f being any of the variables of the system. ω represents the angular frequency and k is the wave number. By substituting (26) into (25), we get the linear system

$$
\begin{pmatrix}
i\omega & -iHk & 0 & 0 & 0 & 0 & 0 \\
-igk & i\omega & 0 & 0 & -ik & 0 & 0 \\
0 & 0 & iH\omega & 0 & -2 & 2 & igH^2k \\
0 & 0 & 0 & iH\omega & 0 & -1 & \frac{1}{2}igH^2k \\
0 & -i\gamma_1\mu Hkc^2 & \gamma_1 c^2 & 0 & iH\omega & 0 & 0 \\
0 & -i\gamma_2\beta Hkc^2 & 0 & \gamma_2 c^2 & 0 & iH\omega & 0 \\
0 & 0 & iB\beta^{-1}Hk & 0 & 0 & 0 & iH\omega
\end{pmatrix}
\cdot
\begin{pmatrix}
\eta_0 \\ u_0 \\ w_0 \\ \xi_0 \\ p_0 \\ q_0 \\ \zeta_0
\end{pmatrix}
= \mathbf{0}.
\tag{27}
$$

As we look for non-trivial solutions, the matrix of the linear system (27) must be singular, yielding the linear dispersion relation:

$$BgH(kH)^2(C_p^4(kH)^2 + 2c^2\gamma_1(gH + 2c^2\beta\gamma_2) - C_p^2(2c^2\gamma_1 + (kH)^2(gH + c^2\gamma_1\mu)))$$

$$2\beta(-C_p^6(kH)^4 + 2c^4gH\gamma_1\gamma_2 + C_p^4(kH)^2(c_2(2\gamma_1 + \gamma_2) + (kH)^2(gH + c2\gamma_1\mu)))$$

$$2\beta(-c^2C_p^2(gH(kH)^2(2\gamma_1 + \gamma_2) + c2\gamma_1\gamma_2(2 + (kH)^2(2\beta + \mu)))) = 0 \tag{28}$$

16

where $C_p = \dfrac{\omega}{k}$ is the phase velocity and we recall that $c^2 = \alpha^2 gH$. Simple manipulations of equation (28) show that for $\alpha^2 \to \infty$, we recover formally the linear dispersion relation satisfied by the original system (22):

$$\frac{C_p^2}{gH} = \frac{1 + B(kH)^2}{1 + \left(\beta + \dfrac{\mu}{2}\right)(kH)^2}. \tag{29}$$

Remark that this dispersion relation corresponds to the full system (22), that is, β and B are parameters to be selected and none of additional assumptions given in Table 1 is made. Therefore, this would be the dispersive relation satisfied by (BMSS), (GN) and (EMS).

Comparing this dispersion relation with the original classical systems, we see that the same one is obtained, which is one of the objectives of the general formulation proposed. In particular, for $\beta = 1/12$, $B \neq 0$, system (22) gives us a generalization of (MS) system introduced in [4], which we have denoted by (EMS). For this particular choice of the parameters, the dispersive relation (29) reduces exactly to the one satisfied by the original system (MS).

Similarly, for $\beta = B = 0$, one recovers the system (BMSS) introduced in [13], which may be seen as an extension of (YKC) introduced in [14] when no additional hypothesis are made. Again the dispersive relation (29) coincides with the original one.

Finally, for $\beta = 1/12$, $B = 0$ we obtain (GN) introduced in [3], which is in fact a generalization of (PER) given in [6] when no additional hypothesis are made. Again the same dispersive relation is obtained.

Figure 2 shows the percent relative error of the phase velocities C_p when compared to the phase velocity given by the Airy theory

$$\frac{C_{Airy}^2}{gH} = \frac{\tanh(kH)}{kH},$$

in a range of $kH \in [0, 4]$. This interval is chosen accordingly to the range in which the original weakly non-linear weakly dispersive systems show a good match with respect to the Stokes linear theory. The value of $B = 1/21$ will be chosen hereinafter as in [4], which minimizes the error for $kH \in [0, 4]$. This can also be observed in Figure 2.

Although we are interested in the formal limit $\alpha \to +\infty$, one could also analyze the exact phase velocity given by (28) for any α. The exact expression of the phase velocity is too tedious and is not given here explicitly. Nevertheless, solving equation (28) will lead to three solutions, corresponding to three phase velocities C_p^{++}, C_p^{+} and C_p^{-}, called the rapid and slow phase velocities respectively. The velocities C_p^{+}, C_p^{++} are always larger than the one obtained for system (22). They do not have any physical meaning and describe the evolution of artificial high-frequency waves related to the modification of the system. It is C_p^{-} the one of interest, which converges to (29) for large values of α.

Figures 3, 4 and 5 show the percent relative error of the phase velocities C_p^{-} when compared with the Airy linear theory for different values of α, as well as the one obtained for system (22).

It can be stated that even for the value of $c = 3\sqrt{gH}$, the linear dispersion relation of the proposed hyperbolic system is quite close to the original one. Therefore not so large values of α are needed in practice, which is good as otherwise a too restrictive CFL condition would be obtained.

5. Numerical scheme

In this Section, we briefly describe the numerical scheme used to discretize the system (24). We shall employ a finite volume method approach. The numerical scheme used here is based on a well-balanced *Polynomial Viscosity Matrix* (PVM) path-conservative scheme (see [29], [30]). A third-order CWENO reconstruction operator in space will be used, combined with a third-order *Total Variation Diminishing* (TVD) Runge-Kutta method in time. Remark that one may choose any other numerical approach suitable for non-conservative hyperbolic systems. This is precisely one of the advantages of (24).

As usual, we consider a set of finite volume cells $\Omega_i = [x_{i-1/2}, x_{i+1/2}]$ that, for the sake of simplicity, we shall consider of constant length Δx, and define

$$\mathbf{U}_i(t) = \frac{1}{\Delta x_i} \int_{\Omega_i} \mathbf{U}(x, t)\, dx,$$
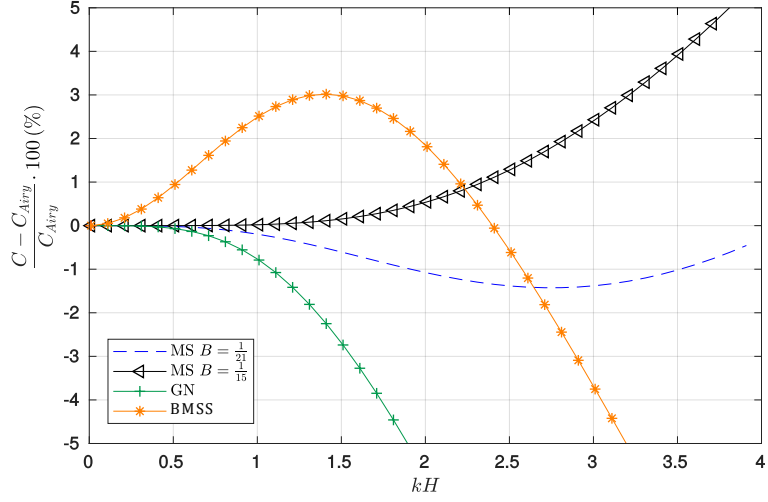
17

Figure 2: Relative error of the phase velocities with respect to the Airy theory for the original systems (MS), (GN), (BMSS).
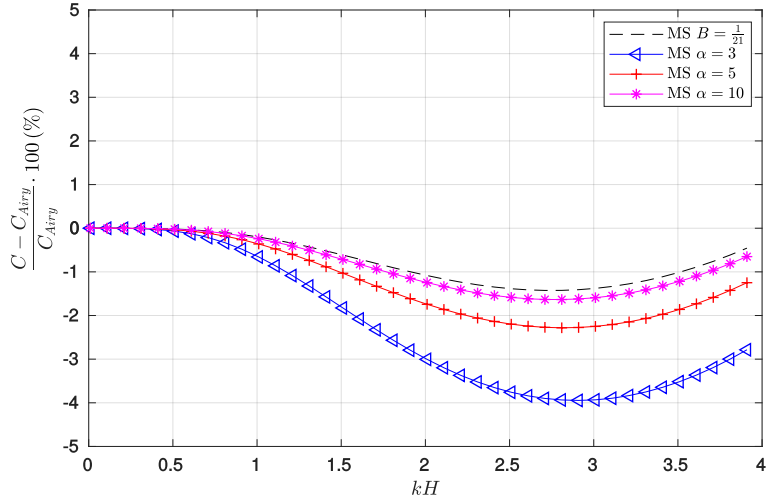

Figure 3: Relative error of the phase velocities with respect to the Airy theory for the original system (MS) (black) and for its new hyperbolic approach (23) ($B = 1/21$, $\beta = 1/12$) using $\alpha = 3$ (blue), $\alpha = 5$ (red) and $\alpha = 10$ (magenta).
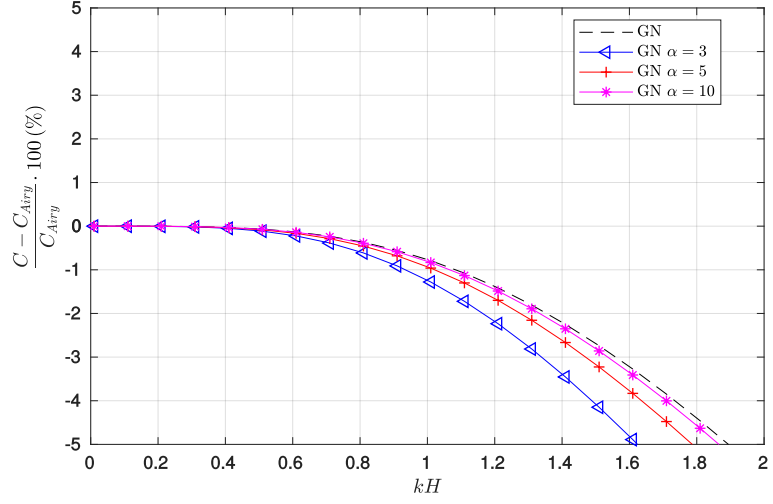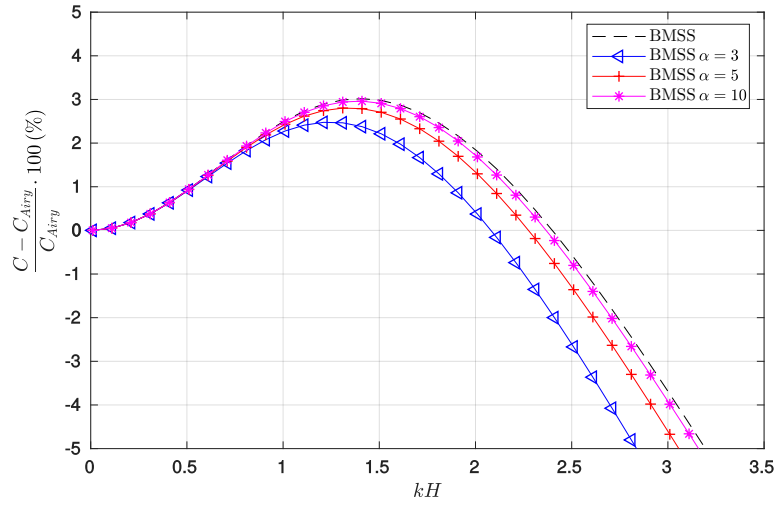
Figure 4: Relative error of the phase velocities with respect to the Airy theory for the original system (GN) (black) and for its new hyperbolic approach (23) ($B = 0$, $\beta = 1/12$) using $\alpha = 3$ (blue), $\alpha = 5$ (red) and $\alpha = 10$ (magenta).

Figure 5: Relative error of the phase velocities with respect to the Airy theory for the original system (BMSS) (black) and for its new hyperbolic approach (23) ($B = \beta = 0$) using $\alpha = 3$ (blue), $\alpha = 5$ (red) and $\alpha = 10$ (magenta).

the cell average of the function $\mathbf{U}(x,t)$ on cell Ω_i at time t. The resulting system (24) can be then recast as an ODE system for the cell averages, which is discretized using a third-order *Total Variation Diminishing* (TVD) Runge-Kutta method [31]. For the sake of clarity, the semi-discrete scheme will be described in what follows, although the third-order in time scheme is used in practice. The source terms $\mathbf{S}(\mathbf{U})$ are discretized semi-implicitly. Thus, in the description of the numerical scheme, they are neglected and only flux and non-conservative products are considered.

The semi-discrete in space high-order path-conservative scheme for the system (24) reads as follows

$$\mathbf{U}'_i(t) = -\frac{1}{\Delta x}\left(\mathcal{D}^-_{i+1/2}(t) + \mathcal{D}^+_{i-1/2}(t) + \mathcal{I}_i(t)\right),$$

where, dropping the dependence on t to relax the notation, $\mathcal{D}^\pm_{i+1/2}$ is given by a PVM path-conservative scheme

$$\mathcal{D}^\pm_{i+1/2} = \frac{1}{2}\left(\mathbf{F}(\mathbf{U}^+_{i+1/2}) - \mathbf{F}(\mathbf{U}^-_{i+1/2}) + \mathbf{B}_{i+1/2}\left(\mathbf{U}^+_{i+1/2} - \mathbf{U}^-_{i+1/2}\right)\right) \pm \frac{1}{2}Q_{i+1/2},$$

$$\mathcal{I}_i = \mathbf{F}(\mathbf{U}^-_{i+1/2}) - \mathbf{F}(\mathbf{U}^+_{i-1/2}) + \int_{\Omega_i} \mathbf{B}[P_{i,\mathbf{U}}(x)]\frac{\partial P_{i,\mathbf{U}}(x)}{\partial x}\,dx.$$

In the expression above $Q_{i+1/2}$ is the numerical viscosity that depends on the choice of the PVM method and $\mathbf{U}^\pm_{i+1/2}$ is defined by a reconstruction procedure on the variables to the left ($^-$) and right ($^+$) of the inter-cell $x_{i+1/2}$. This is done using a reconstruction operator $P_{i,\mathbf{U}}(x)$ and will be described in the next subsection.

The term $\mathbf{B}_{i+1/2}\left(\mathbf{U}^+_{i+1/2} - \mathbf{U}^-_{i+1/2}\right)$ accounts for the path-integral of non-conservative terms. In this work, the simple straight-line segment path for the variables h, η, u, w, ξ, p, q and $h\zeta$ is chosen, and thus the path-integral can be computed exactly using a mid-point quadrature rule, or equivalently:

$$\mathbf{B}_{i+1/2} = \mathbf{B}(\mathbf{U_{i+1/2}}).$$

For example, for the second component of $\mathbf{B}_{i+1/2}\left(\mathbf{U}^+_{i+1/2} - \mathbf{U}^-_{i+1/2}\right)$, it reads:

$$\mathbf{B}_{i+1/2}\left(\mathbf{U}^+_{i+1/2} - \mathbf{U}^-_{i+1/2}\right)_{[2]} = (gh_{i+1/2} + 2\,(p_{i+1/2} - q_{i+1/2}))\left(\eta^+_{i+1/2} - \eta^-_{i+1/2}\right) - 2\,(p_{i+1/2} - q_{i+1/2})\left(h^+_{i+1/2} - h^-_{i+1/2}\right).$$

Finally, $\mathbf{U}_{i+1/2}$ contains the Roe averages of the variables.

The viscosity term $Q_{i+1/2}$ results from the evaluation of a Roe Matrix at $x_{i+1/2}$ by a polynomial that interpolates the absolute value function (see [29]). Here we are using a first-degree polynomial that uses some estimation of the slowest (S_L) and fastest (S_R) wave speeds. With this choice, the numerical scheme coincides with an extension for non-conservative systems of the classical HLL Riemann-solver.

Finally, the volume integral

$$\int_{\Omega_i} \mathbf{B}[P_{i,\mathbf{U}}(x)]\frac{\partial P_{i,\mathbf{U}}(x)}{\partial x}\,dx,$$

is numerically approximated using any Gaussian quadrature rule of the same order of the scheme.

Remark 8. *The first-order numerical scheme considered here is well-balanced for water at rest solutions*

$$\eta = h - H = cst,\ u = w = \xi = p = p_b = \zeta = 0,$$

and linearly $L^\infty-$stable under the usual CFL condition

$$\Delta t < CFL\frac{\Delta x}{|\lambda_{max}|},\quad 0 < CFL \leq 1,\quad |\lambda_{max}| = \max_i\left\{|u_i| + \sqrt{gh_i + p_i\gamma_1\mu c^2},\ |u_i| + \sqrt{B\beta^{-1}gh_i/2}\right\}.$$

Moreover, the scheme is positive preserving for the water height h for a smooth bathymetry H, under $\frac{1}{2}$CFL condition.

Remark 9. *For the test cases shown in the next section, c is chosen proportional to the characteristic celerity $c = \alpha\sqrt{gH_0}$, where H_0 is the characteristic depth of the medium. However, the larger the value of α is, the more restrictive CFL condition we have. In practice, numerical tests show that $\alpha = 3$ is a good choice to keep a good balance between accurate numerical results and dispersion relations (see Figures 3-5).*

Remark 10. *A high-order numerical scheme will be well-balanced and positive preserving, provided a well-balanced and positive preserving reconstruction operator is used (see [32]).*

5.1. High-order scheme based on reconstruction operator

In this subsection, we briefly describe the reconstruction procedure employed in this paper. For a generic scalar variable $v(x)$, given a sequence $\{V_i\}$ of cell averages, an approximation function is calculated inside every cell Ω_i, using the values V_j in a given *stencil*,

$$P_{i,V}(x) = P_i(x; V_{i-l}, \ldots, V_{i+r}),$$

with l, r two natural numbers. The reconstructions at the cell boundaries are then calculated by taking the limits of these functions:

$$\lim_{x \to x_{i-1/2}^+} P_{i,V}(x) = V_{i-1/2}^+, \qquad \lim_{x \to x_{i+1/2}^-} P_{i,V}(x) = V_{i+1/2}^-.$$

In order to have a reconstruction operator which is well-balanced for water at rest solutions, the following strategy may be followed. Starting from a sequence

$$\left\{ h_j, hu_j, hw_j, h\xi_j, hp_j, hq_j, h\zeta_j, H_j \right\}_{j=i-l}^{i+r}$$

of cell values, consider the new sequence

$$\left\{ h_j, hu_j, hw_j, h\xi_j, hp_j, hq_j, h\zeta_j, \eta_j \right\}_{j=i-l}^{i+r},$$

where $\eta_j = h_j - H_j$, and apply the reconstruction operator to obtain polynomials

$$P_{i,h}, \; P_{i,hu}, \; P_{i,hw}, \; P_{i,h\xi}, \; P_{i,hp}, \; P_{i,hq}, \; P_{i,h\zeta}, \; P_{i,\eta};$$

then define

$$P_{i,H} = P_{i,h} - P_{i,\eta}.$$

This reconstruction is exactly well-balanced for stationary solutions corresponding to water at rest if the reconstruction operator is exact for constant functions. In this paper we will consider the CWENO3 reconstruction with the optimal definition of the nonlinear weights (see [33] for more details). Therefore, we propose here an explicit finite volume and well-balanced numerical method of third-order accuracy in both space and time.

5.2. Numerical treatment of wet-dry fronts

A wet-dry treatment, as described in [17], [34], in regions with emerging bottom is considered in the numerical scheme. No special treatment is required for the non-hydrostatic pressure as usual, since in the presence of wet-dry fonts it vanishes automatically. The key to the numerical treatment for wet-dry fronts with emerging bottom topographies relies on:

- The computation of the gradient of η for emerging bottoms is carried out as in [34] to avoid spurious pressure forces.

- To compute velocities (such as u) from the discharges (hu), very small values for the water height h may appear. To overcome the difficulties due to large round-off errors in computing velocities, we define them as in [35], applying the desingularization formula

$$u = \frac{\sqrt{2}hhu}{\sqrt{h^4 + \max(h^4, \epsilon^4)}}, \tag{30}$$

which gives the exact value of u for $h \geq \epsilon$, and gives a smooth transition of u to zero when h tends to zero without truncation. In this work we set $\epsilon = 10^{-5}$ for the numerical tests. A more detailed discussion about the desingularization formula can be seen in [35].

For the numerical tests studied in the next section, boundary conditions (BC) are imposed weakly, by enforcing suitable relations at virtual exterior nodes, at each boundary.

Nevertheless, to mimic free-outflow boundary conditions, reflections at the boundaries might perturb the numerical solution at the inner domain. As in many other works (see [27], [36], [37], [38] among others), this condition is supplemented here with an absorbing BC. This is done by using a relaxation zone method similar to the one proposed in [38]. Absorption of waves is achieved by simply defining a relaxation coefficient $0 \leq m(x) \leq 1$.

Given a width L_{Rel} of the relaxation zone, the solution within the relaxation zone is then redefined to be

$$\widetilde{\mathbf{U}}_i = m_i \mathbf{U}_i$$

for every i in the relaxation zone. m_i is defined as

$$m_i = \sqrt{1 - \left(\frac{d_i}{L_{Rel}}\right)^2},$$

where d_i is the distance between the centre of the cells I_i to the closest boundary. In our numerical experiments we set

$$L \leq L_{Rel} \leq 1.5L,$$

being L the typical wavelength of the outgoing wave.

6. Numerical tests

In this section we intend to exhibit the ability of the proposed general hyperbolic formulation (23) to deal with and correctly represent a wide variety of complex situations involving dispersive water waves over wet-dry fronts or emerging topographies; breaking waves; propagation, shoaling and inundation of solitary waves; among others.

In order to validate the general formulation and its hyperbolic approximation proposed in this paper, we will show comparisons with laboratory data as well as some standard numerical test for dispersive systems. We provide comparisons between the numerical results from the original systems (BMSS) ($B = \beta = 0$), (GN) ($B = 0$, $\beta = 1/12$), (MS) ($B = 1/21$, $\beta = 1/12$), and their hyperbolic approximations given by (23) and the corresponding parameters B and β that will be tagged in the following with (H-BMSS), (H-GN) and (H-EMS) respectively. For the case of the (MS) comparisons, we sometimes supplement with numerical simulations of the hyperbolic system (23) with $B = 1/21$, $\beta = 1/12$, and making some assumptions to be detailed, tagged as (H-MS).

Concerning the numerical results corresponding to the discretization of the original Boussinesq-type systems, here we employ the ideas raised in [17] and in [22] to numerically approximate them. Remark that these Boussinesq-type systems have already been validated in different works (see [14], [17], [18], [19], [20], [21], [22], [36], [37], [39] and references therein).

In what follows, the gravity acceleration is set to $g = 9.81$. The relaxation parameter is set to $\alpha = 3$. A Manning coefficient of $n_m = 0.01$ is used to define the glass surface roughness used in the experiments. The breaking criteria is considered with the parameters $b_1 = 0.5$, $b_2 = 0.15$ as it was already mentioned in Subsection 3.2. Similarly, as it was mentioned in Subsection 5.2, the parameter value appearing in the desingularization formula (30) is set to $\epsilon = 10^{-5}$. Finally, in all test cases the initial condition for the auxiliary variable ζ is numerically approximated as $\zeta(x, 0) = B\partial_x\eta_0(x)$, η_0 being the corresponding initial condition for the free-surface variable η. This is done using finite differences of fourth-order. All the quantities are expressed in units of measure of the International System of Units.

6.1. Order of accuracy

In this test, we take as an initial condition a solitary wave of amplitude $A = 0.1$ over a flat bottom $H = 1$. To do that, we use the analytical solution for the system (BMSS) given in [13] as an approximate solitary wave solution for the hyperbolic system (H-BMSS) (see also [18]). Similarly, we employ the analytical solution for the system (GN) given in [13] as an approximate solitary wave solution for the hyperbolic system (H-GN). Finally, in the case of the

system (H-EMS), we employ the same exact solitary wave as for the (GN) system, since both systems share a closer dispersion relation.

From the previous indications, we define the initial condition for the variables h, hu, hw, and hp. Then, for a flat bottom, using Remark 4 as well as the very definition of ζ, we have that the remaining variables $h\xi$, hq and $h\zeta$ can be computed as

$$h\xi = \frac{\beta}{\mu}hw, \qquad hq = \frac{1}{\mu + 2\beta}\left(2\beta hp - \frac{1}{2}(\mu - 2\beta)gh^3\partial_x\zeta\right), \qquad h\zeta = h\partial_x\eta. \tag{31}$$

The exact solutions of the hyperbolic systems are not known, but reference solutions are computed with the third-order scheme and 12800 cells. Periodic boundary conditions are imposed and the computational domain is $\Omega = [-150, 150]$. The third-order scheme is run with an increasing number of cells and the errors for some of the variables of the system are computed. The integration time is $T = 1$, and the CFL number is set to 0.4.

Table 2 shows the errors and the convergence rates for the more challenging case of the system (H-EMS). Table 2 shows a perfect agreement with the expected values showing that the theoretical order of accuracy is achieved.

N	L^1 error h		L^1 error hu		L^1 error hw		L^1 error hp		L^1 error $h\zeta$	
800	3.03e-04	–	9.29e-04	–	5.70e-04	–	2.58e-03	–	1.63e-05	–
1600	3.87e-05	2.97	1.22e-04	2.93	6.78e-05	3.07	2.99e-04	3.11	2.08e-06	2.96
3200	4.80e-06	3.01	1.55e-05	2.97	7.65e-06	3.15	3.52e-05	3.09	2.58e-07	3.02
6400	5.34e-07	3.17	1.80e-06	3.11	7.39e-07	3.37	3.95e-06	3.16	2.85e-08	3.18

Table 2: Accuracy test. L^1 numerical errors and convergence rates.

6.2. Still water steady-state

In this test we consider the same domain and boundary conditions as in the previous test. The bathymetry H is given by

$$H(x) = 1 - 0.9e^{-x^2}.$$

We consider the initial condition given by

$$h_0(x) = H(x), \quad hu_0(x) = hw_0(x) = h\xi_0(x) = hp_0(x) = hq_0(x) = h\zeta_0(x) = 0.$$

The exact solution is a steady-state with still water, coinciding at all times with the initial condition. Table 3 shows the errors observed at time $T = 100$, with a CFL number set to 0.9. It clearly shows that the scheme is well-balanced since these are all of the order of the machine precision.

6.3. Comparison between classical models and the new approach presented in this paper

We shall compare the general system (22) for different values of B and β, using the hyperbolic approach, with the corresponding original counterpart. To do so, we propose an idealized case of waves that propagates over two bumps. An emerging bathymetry is included for the simulation of shoreline processes such as shoaling, breaking of the waves and run-up. The bathymetry is given by

$$H(x) = 1 - 0.2e^{-x^2/20} - 0.6e^{-(x+50)^2/60} - 1.75e^{-(x-100)^2/800},$$

and the domain channel is $\Omega = [-115, 115]$, discretized into cells of $\Delta x = 0.2$ length. We shall consider the still water reference level at $z = 0$ so that the bottom emerges. We then perturb the free-surface by adding a wave at $x = 0$ and define the initial water thickness by

$$h_0(x) = \max\{H + 0.75e^{-x^2/1.25}, 0\},$$

23

N	L^1 error η	L^1 error hu	L^1 error hw	L^1 error hp	L^1 error $h\zeta$
80	2.55e-16	2.38e-15	1.45e-15	4.81e-15	1.36e-16
160	2.13e-16	2.98e-15	1.50e-15	4.95e-15	1.38e-16
320	3.59e-16	2.71e-15	2.25e-15	9.72e-15	2.21e-16
640	1.93e-16	8.12e-16	7.45e-16	5.93e-15	1.38e-16

Table 3: Well-balancing errors for the still water steady states.

in other words, the free-surface is given by $\eta_0 = 0.75e^{-x^2/1.25}$ up to the point where the bottom emerges. The rest of the flow variables are set initially to zero, except for $\zeta(x,0) = B\partial_x\eta_0$. The integration time is $T = 25$, and the CFL number is set to 0.9. For this numerical test the breaking mechanism is turned off in order to make the fairest comparisons between the different models.

In the beginning, the initial water surface elevation is released and split into two waves that travel in opposite directions trying to leave the domain. The first bump situated at the bathymetry at $x = 0$, force the appearance of the first high harmonic waves, and once they travel over the second bump, the waves split into higher harmonics. This evidence can be observed in nature, as it can be seen in [40] where a generated wave train travels over a submerged bar that force the appearance of higher harmonic waves.

In Figures 6 and 7 we show the snapshots at different times of the result obtained with the hyperbolic models (H-BMSS) and (H-GN), compared with their original systems. The comparison between the originals and the approximated hyperbolic models show excellent agreement, even for the small value of $\alpha = 3$, covering the propagation, shoaling, generation of non-linear higher harmonics and run-up.

Figure 8 shows the same comparison, as described above, between the genuine system (MS) derived by Madsen et al in [4] and the hyperbolic system (H-EMS). Here we can observe more discrepancies, even though the two leading waves are captured by the hyperbolic system with a reasonable error in both amplitude, frequency, and position. The run-up is also well captured when comparing both simulations. These discrepancies can be explained from the assumptions made in the derivation of the original system (MS) in [4], which have not been considered here.

Consequently, we have considered a comparison with the hyperbolic system (23) with $\beta = 1/12$, $B = 1/21$, which corresponds to the (MS) system neglecting convective terms $\partial_x(uhw) = \partial_x(uh\xi) \approx 0$, as well as by substituting h by H in the equations (23c)-(23g) and in the term $\partial_x(hp)$ in equation (23b). This corresponds to the same substitutions performed in the original (MS) system, and results in the fairest comparison between the original (MS) system and a hyperbolic approach. The results are shown in Figure 9. Figure (10) shows a zoomed snapshot at $t = 10$ and $t = 25$ where the aforementioned discrepancies can be better observed.

6.4. Head-on collision of two solitary waves

The head-on collision of two equal solitary waves is a common test for the Boussinesq-type models (see [17], [21], [22], [37]). Neglecting viscosity effects, the collision of the two waves is comparable to the reflection of one wave by a vertical wall. After the interaction, one should ideally recover the initial profiles. This numerical test presents additional challenges to the model due to the abrupt change of the non-linear and frequency dispersion characteristics.

The initial condition consists of two solitary waves of equally amplitude $A = 0.2$, given as in Subsection 6.1, propagating on a depth of $H = 1$ in opposite directions. The waves are initially placed at $x = 50$ and $x = 150$. The domain $\Omega = [0, 200]$ is discretized with $\Delta x = 0.1$. Finally, free-outflow boundary conditions are considered and the CFL number is set to 0.9. Figure 11 shows the entire evolution of the two solitary waves. After the collision, both waves maintain the initial amplitude and the same speed but in opposite directions as expected. An excellent agreement can be observed at the final time, after the collision. Figure 12 shows a detailed comparison of the computed and exact solitary wave solutions at the right boundary for the free-surface at time $T = 100/v_A$, where $v_A = \sqrt{g(A + H)}$ is the propagation velocity of the solitary wave.
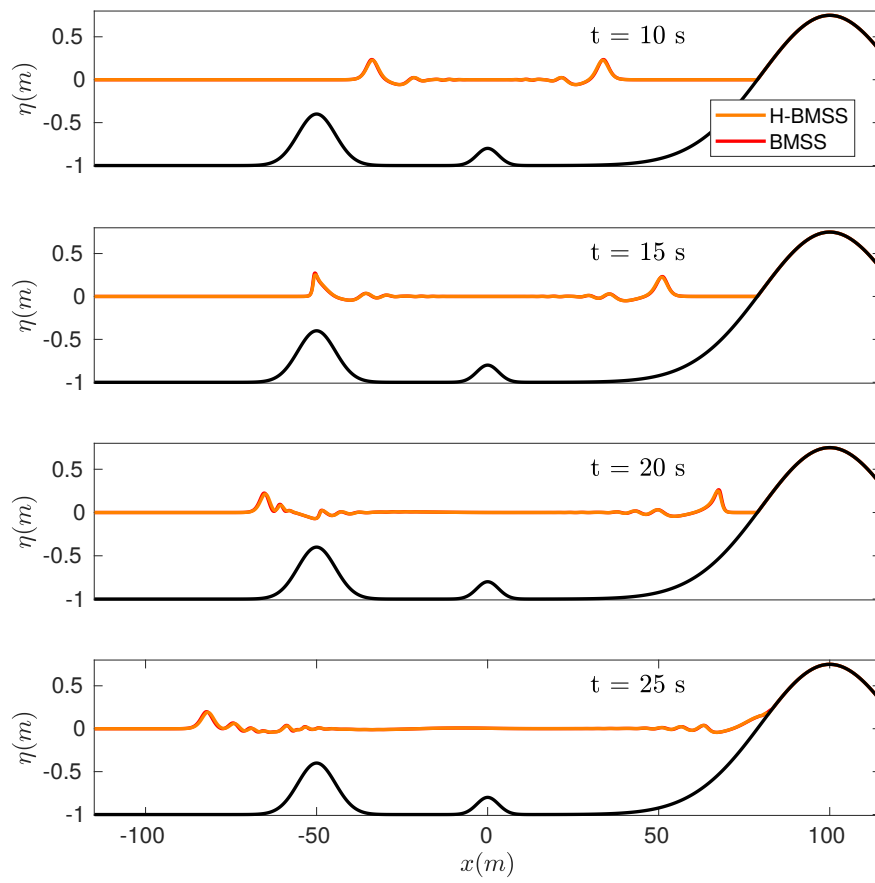
Figure 6: Comparison of the computed free-surfaces from the system (BMSS) (red) and from the proposed hyperbolic approximation (H-BMSS) (orange).
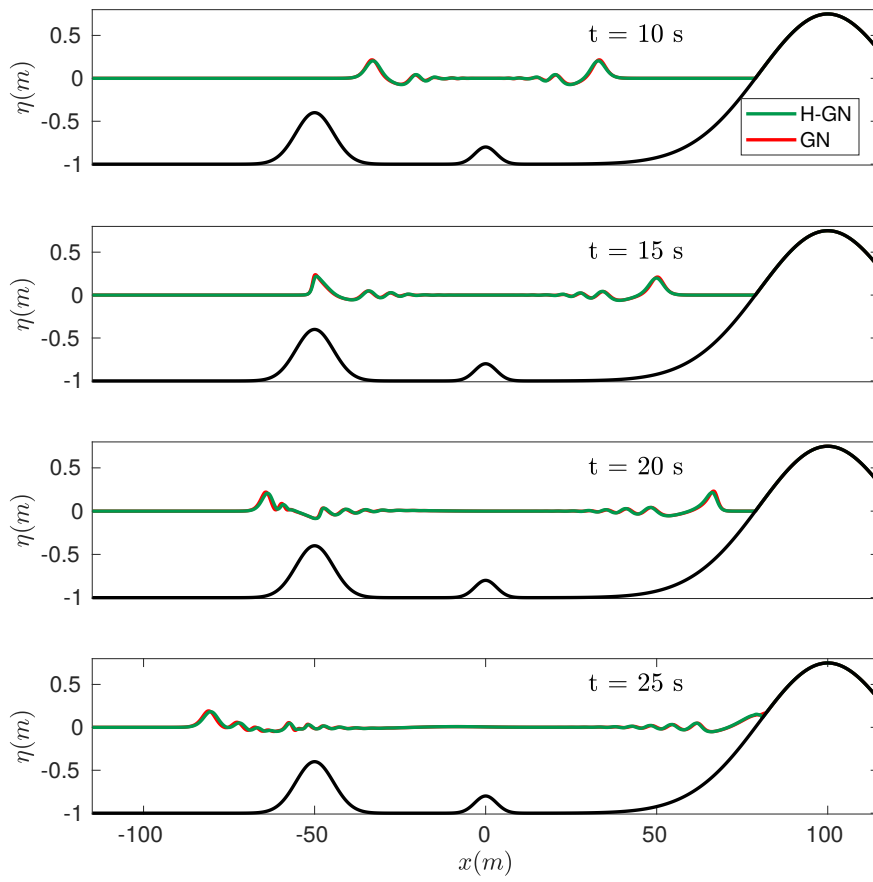
Figure 7: Comparison of the computed free-surfaces from the system (GN) (red) and from the proposed hyperbolic approximation (H-GN) (green).
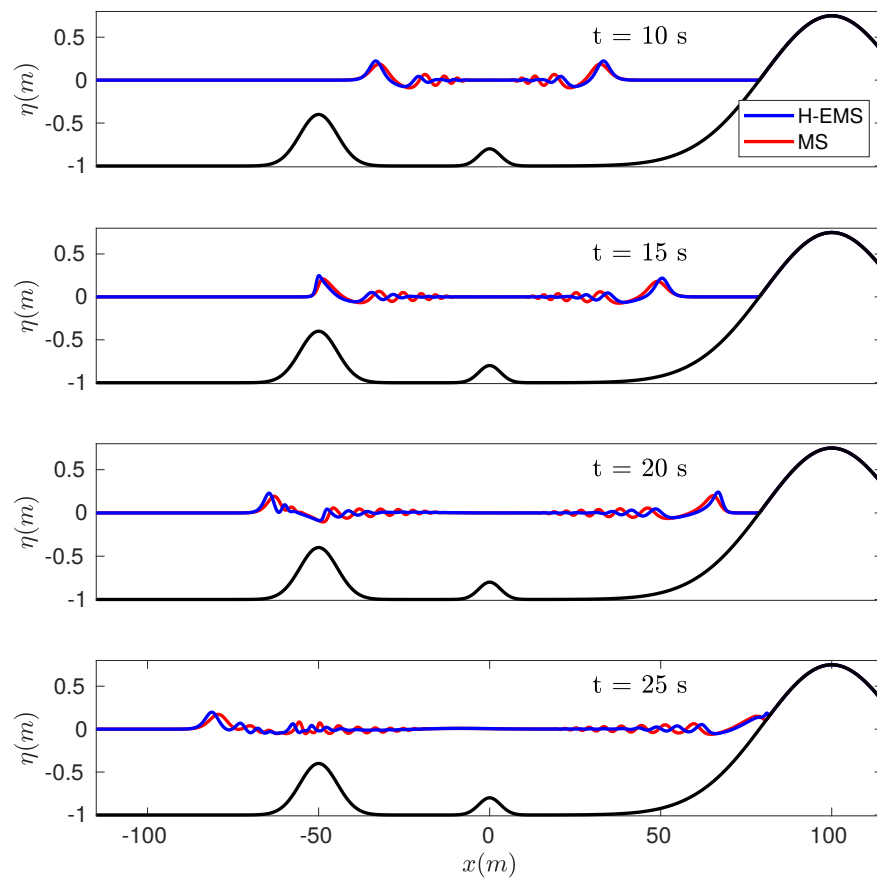
Figure 8: Comparison of the computed free-surfaces from the system (MS) (red) and from the proposed hyperbolic approximation of the (MS) extension (H-EMS) (blue).
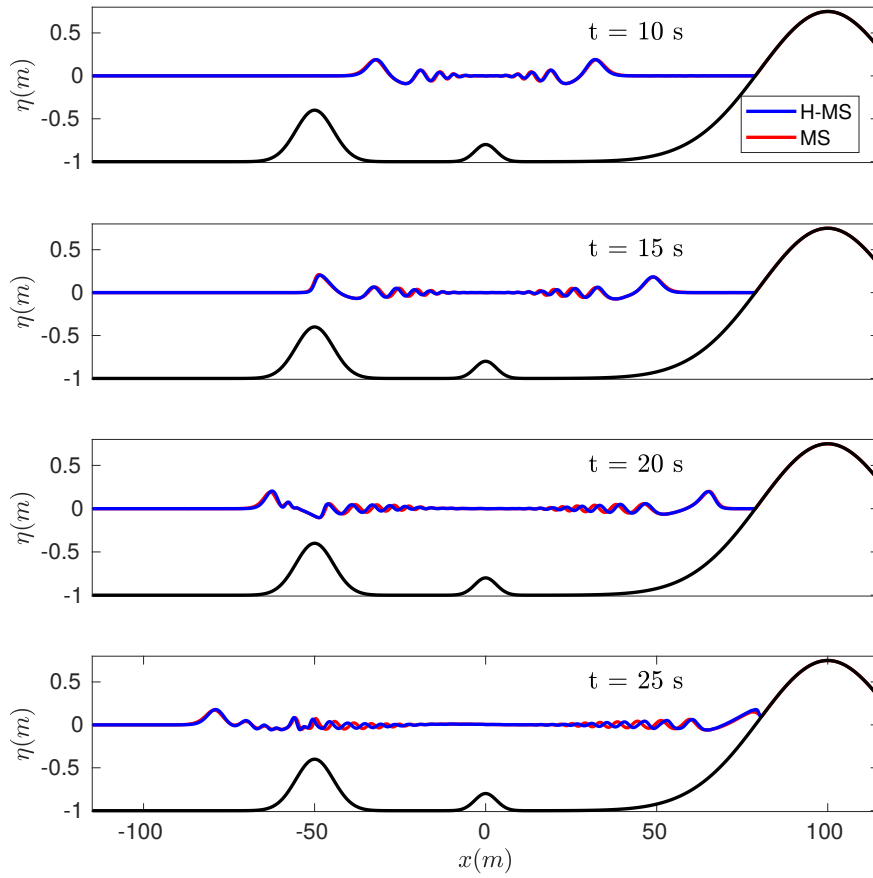
Figure 9: Comparison of the computed free-surfaces from the system (MS) (red) and from the proposed hyperbolic approximation (H-MS) neglecting the convective terms $\partial_x(uhw) = \partial_x(uh\xi) \approx 0$ and substituting h by H in (23c)-(23g) (blue).
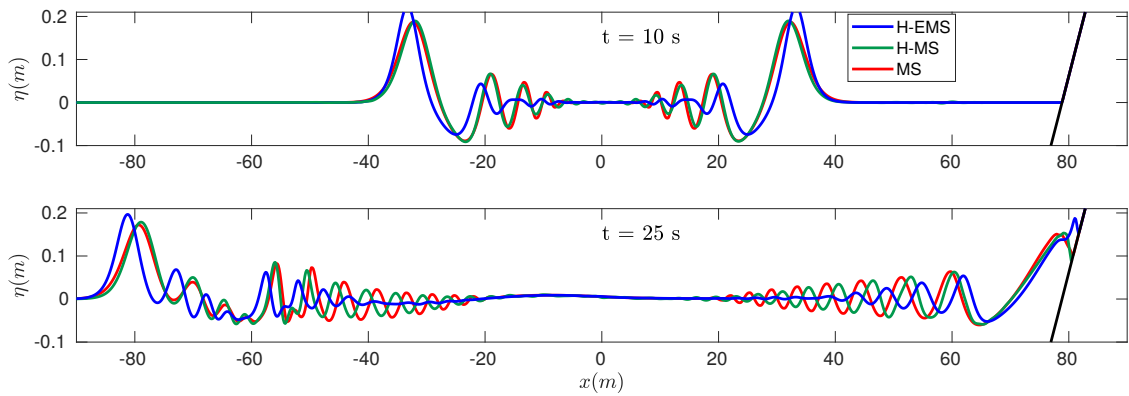
Figure 10: Comparison of the computed free-surface from the system (MS) (red), the hyperbolic extension (H-EMS) (blue) and from the proposed hyperbolic (H-MS) (green) at time $t = 10$ and $t = 25$.
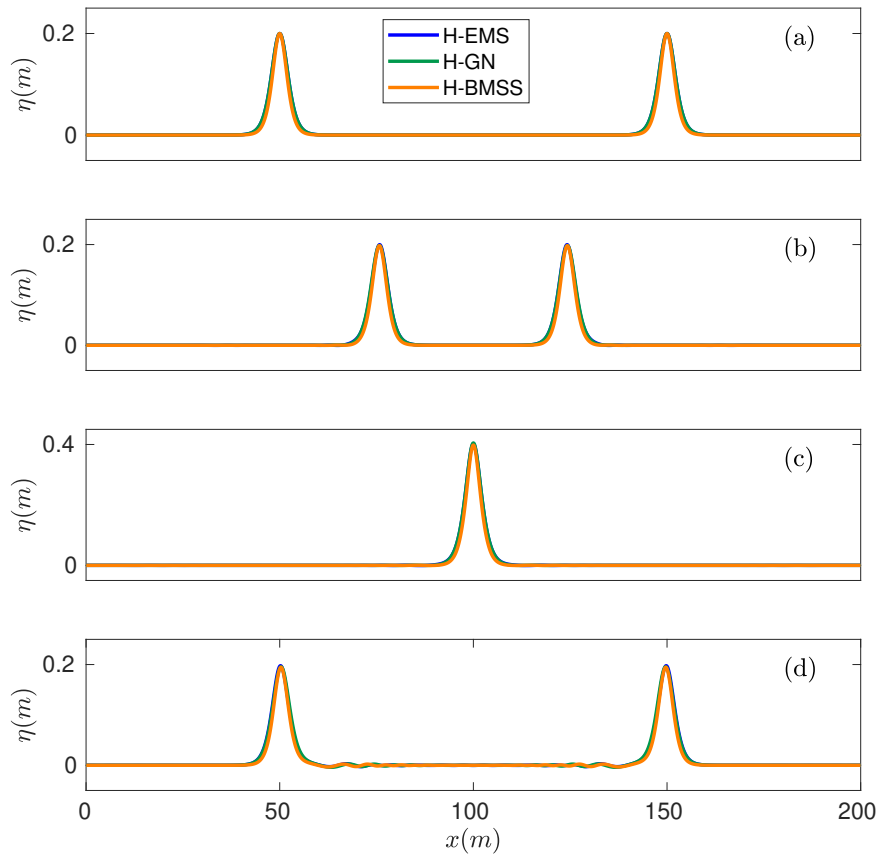
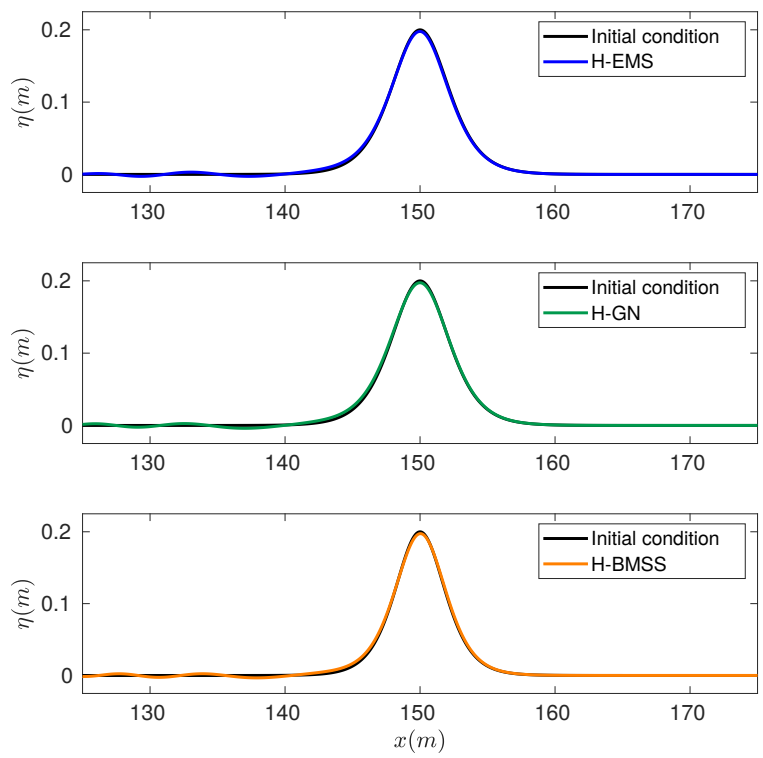Figure 11: Head-on collision of two solitary waves at times $T\sqrt{g(A+H)} = 0,\ 25,\ 50,\ 100$.

Figure 12: Zoom of Head-on collision of two solitary waves at time $T\sqrt{g(A+H)} = 100$.
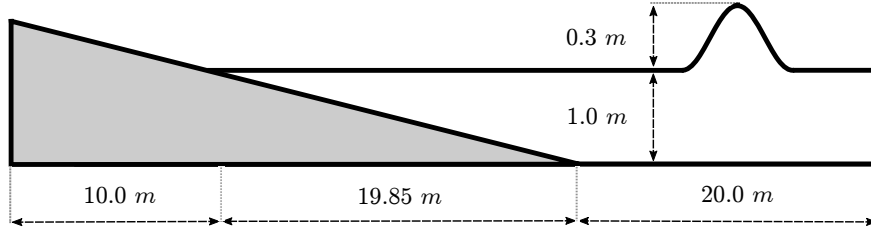
Figure 13: Sketch of the bathymetry used for the solitary wave run-up onto a beach test problem.

Thus, this numerical test also evinces the ability of the numerical approach proposed in this paper to correctly propagate solitary waves over flat bottoms.

6.5. Solitary wave run-up on a plane beach

Synolakis [41] carried out laboratory experiments for incident solitary waves, to study propagation, breaking and run-up over a planar beach with a slope 1 : 19.85. Many researchers have used this data to validate numerical models (see [17], [18], [21], [22], [36], [37] among others). With this test case, we assess the ability of the model to describe shoreline motions and wave breaking, when it occurs. Experimental data are available in [41] for surface elevation at different times. The bathymetry of the problem is described in Figure 13. A solitary wave of amplitude $A = 0.3$, given as in Subsection 6.1 is placed at the location $x = 20$. This serves as initial condition for the free-surface elevation and all other flow quantities. The computational domain $\Omega = [-10, 40]$ is divided into cells of length $\Delta x = 0.1$. Free-outflow boundary conditions are considered and the CFL number is set to 0.9.

Figure 14 shows snapshots at different times corresponding to $T\sqrt{g/H} = 15, 20, 25, 30$ (here we are using $H = 1$). Comparison between experimental and simulated data is shown for the systems (H-MS), (H-GN), (H-BMSS) and (SWE), which stands for hydrostatic simulations (non-linear shallow water equations, see Remark 7).

Figure 14 also shows, between vertical bars, the region where the breaking mechanism is active. Numerical results also evince small discrepancies for the different systems. Some of this differences may be expected in view of the dispersive relation celerity shown in Figure 2. Systems (H-GN) and (H-EMS) tend to decelerate waves which results in the later time of arrival for the wave. The simulations highlight as well the importance of dispersive effects when compared with hydrostatic simulations (SWE).

In addition, good results are obtained for the maximum wave run-up, where the friction terms play an important role. Note that no additional wet-dry treatment for the non-hydrostatic pressure is needed. This test shows that the proposed hyperbolic strategy, the chosen breaking mechanism, as well as the standard SWE friction term, perform adequately for the proposed hyperbolic systems. Moreover, the corresponding discretization is robust and can deal with the presence of wet-dry fronts correctly.

6.6. Waves generated by an impulsive bed up-thrust

Let us consider now a laboratory test with a moving bottom configuration. We shall consider the wave generation produced by an impulsive exponential bottom movement. This experiment was studied previously (analytically and experimentally) by Hammack in [42] and later tested by Fuhrman et al in [43] by means of a high-order Boussinesq-type system. The experiment considers an impulsive exponential bed up-thrust described by

$$H(x, t) = H_0 - A(1 - e^{-1.11t/t_c})\mathcal{H}\left(b^2 - x^2\right),$$

where $\mathcal{H}$ is the Heaviside step function and $H_0 = 0.9$. Here $A = 0.1$, $b = 12.2$ and $t_c = 0.148b/\sqrt{g(A + H)}$ are the three parameters that characterize the bed displacement: an amplitude of movement A, a characteristic size b, and a characteristic time t_c (see [42]). Here we supplement the impulsive bed condition with a lake-at-rest steady state initial condition, that is, h corresponds to the still water depth and the rest of the flow variables are initially set to zero, including $\zeta_0 = B\partial_x\eta_0 = 0$. A domain $\Omega = [-100, 500]$ discretized with $\Delta x = 0.1$ is considered and free-outflow boundary conditions are imposed. The CFL number is set to 0.9.
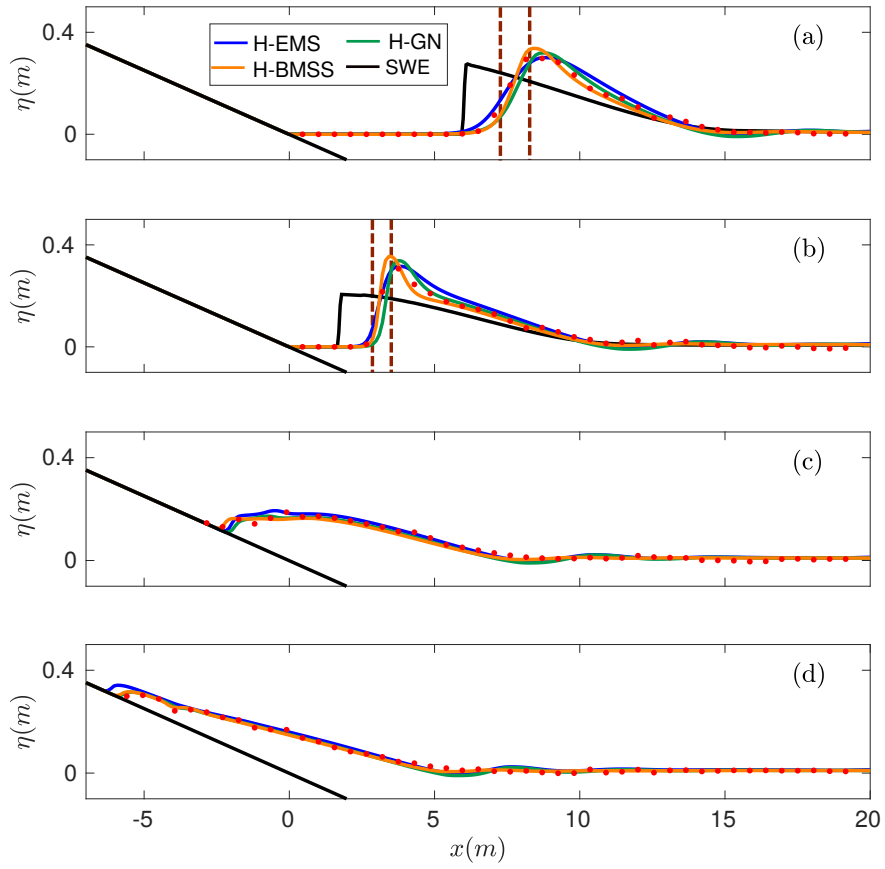
31

Figure 14: Comparison of experiments data (red) and simulated ones with the proposed hyperbolic systems during the run-up at times $T\sqrt{g/H} = 15, 20, 25, 30$. Between bars, regions where breaking mechanism is active are shown.
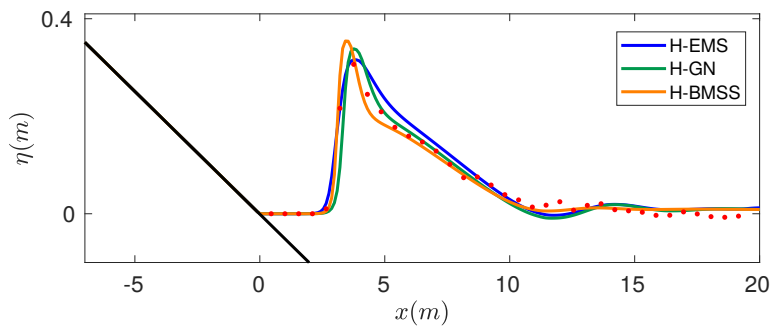

Figure 15: Comparison of experiments data (red) and simulated ones with the proposed hyperbolic systems at time $T\sqrt{g/H} = 20$.
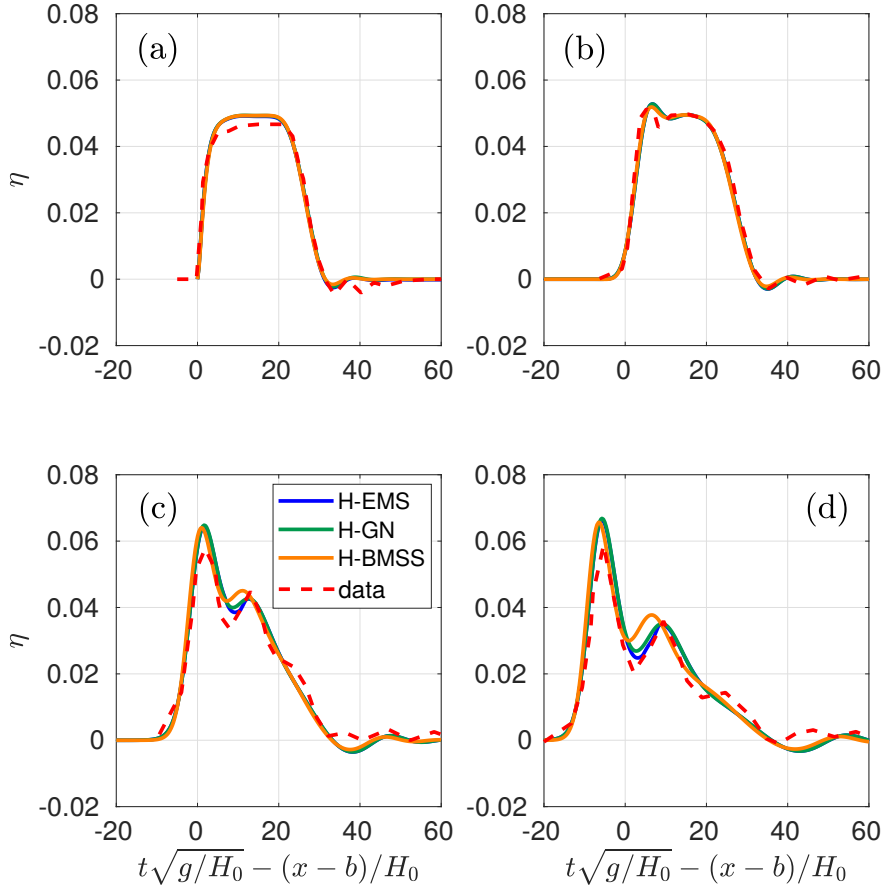
Figure 16: Time series of surface elevations from the hyperbolic systems (full line) and experiments (dashed line, from Hammack) at locations (a) $(x - b)/H_0 = 0$, (b) 20, (c) 180, and (d) 400.

Time series at different points from [42] are presented in Figure 16. In general, Figure 16 shows a good, though not perfect, agreement between the computed and the observed time series. The differences start being noticeable from the beginning (see (*a*) in Figure 16), near the generation. Here the free-surface is overestimated by the numerical models when compared to the experimental data. The discrepancies are not so strong in (*b*), further away from the generating source. Then (*c*) and (*d*) show that the waves given by the models are similar in shape to the experimental data. The peaks are a little bit overestimated with respect to the experimental data but they are in general placed at the correct time. Nevertheless, the position of the second peak for (BMSS) is not so good. The results are in agreement with the observations made by other authors as in [43]. Remark that (H-EMS), which has the most accurate dispersive relation, gives the best agreement.

These results confirm the ability of the hyperbolic systems introduced in this paper to model shallow dispersive waves coming from underwater earthquake type events. Moreover, the natural extension to the case of non-stationary bathymetry for the (H-EMS) model provided here has turned out to perform adequately in such situations.

7. Conclusion

A novel first-order reformulation of classical Boussinesq-type models for shallow non-hydrostatic free-surface flows has been proposed. The aim is to incorporate dispersive effects in the propagation of waves in a homogeneous, inviscid and incompressible fluid.

The new reformulation collects the main Boussinesq-type dispersive systems and it even allows to propose generalizations of them, by including missing terms that were neglected during their derivation. It allows also to easily take into account the effects of a time-dependent bathymetry that was not considered originally. The new system has the following advantages:

First, it covers in a simple and general way the main well-known dispersive shallow water systems that are used in ocean engineering. The equivalence with the different models is done by means of two free parameters and eventually, some additional assumptions (see Table 1).

Second, a single numerical approach may be proposed which will result in providing a unified implementation of the leading dispersive systems. Moreover, the proposed reformulation consists of a first-order PDE system. This results in an advantage when designing numerical schemes. On the one hand, it makes simple the implementation of the numerical schemes. It allows as well to obtain more efficient computations, due to the absence of high-order derivatives, reducing the numerical stencil needed. On the other hand, it avoids several and challenging situations involving the design of robust, well-balanced and positive preserving numerical schemes for high-order PDEs.

Finally, the system (22) has been solved numerically by means of relaxed hyperbolic system (23) that formally converges to the original one. The dispersion properties of this new hyperbolic system are close to those of the aforementioned original model (see Figures 3-5). The most important advantage of this new hyperbolic formulation is that it can be easily discretized with explicit and high-order accurate numerical schemes for hyperbolic systems. Here, a third-order finite volume scheme based on a CWENO reconstruction and a path conservative PVM method has been proposed. Nevertheless, any numerical scheme for non-conservative hyperbolic systems such as Discontinuous Galerkin schemes among others can also be considered.

We have presented different numerical tests: academic examples, accuracy, and well-balanced test, comparison with experimental data, and run-up processes in wet-dry areas near the shore, etc. The numerical approach works well and provides a good approximation. Comparisons with the original Boussinesq-type systems that are approximated show excellent results.

The proposed model and the numerical scheme presented in this work provide thus a general, efficient and accurate approach to model dispersive effects in the propagation of waves near coastal areas and intermediate waters.

8. Acknowledgements

References

[1] M. B. Abbott, A. D. McCowan, I. R. Warren, Accuracy of Short Wave Numerical Models, Journal of Hydraulic Engineering 110 (1984) 1287–1301.

[2] J. Boussinesq, Théorie des ondes et des remous qui se propagent le long d'un canal rectangulaire horizontal, en communiquant au liquide contenu dans ce canal des vitesses sensiblement pareilles de la surface au fond., Journal de Mathématiques Pures et Appliquées 17 (1872) 55–108.

[3] A. E. Green, P. M. Naghdi, A derivation of equations for wave propagation in water of variable depth, Journal of Fluid Mechanics 78 (1976) 237–246.

[4] P. A. Madsen, O. R. Sørensen, A new form of the Boussinesq equations with improved linear dispersion characteristics. Part 2. A slowly-varying bathymetry, Coastal Engineering 18 (1992) 183–204.

[5] O. Nwogu, Alternative form of Boussinesq equations for nearshore wave propagation, Journal of Waterway, Port, Coastal and Ocean Engineering 119 (1993) 618–638.

[6] D. H. Peregrine, Long waves on a beach, Journal of Fluid Mechanics 27 (1967) 815–827.

[7] M. F. Gobbi, J. T. Kirby, G. Wei, A fully nonlinear Boussinesq model for surface waves. Part 2. Extension to O(kh)4, Journal of Fluid Mechanics 405 (2000) 181–210.

[8] G. B. Whitman, Linear and nonlinear waves., Earthquake Engng. Struct. Dyn. 4 (1974) 518.

[9] J. M. Witting, A unified model for the evolution of nonlinear water waves., Journal of Computational Physics 56 (1982) 203–236.

[10] M. F. Gobbi, J. T. Kirby, G. Wei, A fully nonlinear Boussinesq model for surface waves. Part 2. Extension to O(kh)4, Journal of Fluid Mechanics 405 (2000) 181–210.

[11] V. Casulli, A semi-implicit finite difference method for non-hydrostatic free surface flows, Numerical Methods in Fluids 30 (1999) 425–440.

[12] G. Stelling, M. Zijlema, An accurate and efficient finite-difference algorithm for non-hydrostatic free-surface flow with application to wave propagation, International Journal for Numerical Methods in Fluids 43 (2003) 1–23.

[13] M.-O. Bristeau, A. Mangeney, J. Sainte-Marie, N. Seguin, An energy-consistent depth-averaged Euler system: Derivation and properties, Discrete and Continuous Dynamical Systems Series B 20 (2015) 961–988.

[14] Y. Yamazaki, Z. Kowalik, K. F. Cheung, Depth-integrated, non-hydrostatic model for wave breaking and run-up, International Journal for Numerical Methods in Fluids 61 (2009) 473–497.

[15] E. D. Fernández-Nieto, M. Parisot, Y. Penel, J. Sainte-Marie, A hierarchy of dispersive layer-averaged approximations of Euler equations for free surface flows, Communications in Mathematical Sciences 16 (2018) 1169–1202.

[16] A. Jeschke, G. K. Pedersen, S. Vater, J. Behrens, Depth-averaged non-hydrostatic extension for shallow water equations with quadratic vertical pressure profile: equivalence to Boussinesq-type equations, International Journal for Numerical Methods in Fluids 84 (2017) 569–583.

[17] C. Escalante, T. Morales de Luna, M. J. Castro, Non-hydrostatic pressure shallow flows: GPU implementation using finite volume and finite difference scheme, Applied Mathematics and Computation 338 (2018) 631–659.

[18] C. Escalante, M. Dumbser, M. J. Castro, An efficient hyperbolic relaxation system for dispersive non-hydrostatic water waves and its solution with high order discontinuous Galerkin schemes, Journal of Computational Physics 394 (2019) 385–416.

[19] D. Lannes, P. Bonneton, Derivation of asymptotic two-dimensional time-dependent equations for surface water wave propagation, Physics of Fluids 21 (2009).

[20] R. Cienfuegos, E. Barthélemy, P. Bonneton, A fourth-order compact finite volume scheme for fully nonlinear and weakly dispersive Boussinesq-type equations. Part I: Model development and analysis, International Journal for Numerical Methods in Fluids 51 (2006) 1217–1253.

[21] V. Roeber, K. F. Cheung, M. H. Kobayashi, Shock-capturing Boussinesq-type model for nearshore wave processes, Coastal Engineering 57 (2010) 407–423.

[22] C. Escalante, E. D. Fernández-Nieto, T. Morales de Luna, M. J. Castro, An Efficient Two-Layer Non-hydrostatic Approach for Dispersive Water Waves, Journal of Scientific Computing 79 (2019) 273–320.

[23] C. D. Munz, P. Omnes, R. Schneider, E. Sonnendrücker, U. Voß, Divergence Correction Techniques for Maxwell Solvers Based on a Hyperbolic Model, Journal of Computational Physics 161 (2000) 484–511.

[24] A. Dedner, F. Kemm, D. Kröner, C. D. Munz, T. Schnitzer, M. Wesenberg, Hyperbolic divergence cleaning for the MHD equations, Journal of Computational Physics 175 (2002) 645–673.

[25] Manning R., On the flow of water in open channels and pipes, Transactions of the Institution of Civil Engineers of Ireland 20 (1891) 161–207.

[26] P. Lynett, P. L. Liu, A two-layer approach to wave modelling, Proceedings of the Royal Society A: Mathematical, Physical and Engineering Sciences 460 (2004) 2637–2669.

[27] D. Lannes, F. Marche, A new class of fully nonlinear and weakly dispersive Green-Naghdi models for efficient 2D simulations, Journal of Computational Physics 282 (2015) 238–268.

[28] H. A. Schäffer, P. A. Madsen, Further enhancements of Boussinesq-type equations, Coastal Engineering 26 (1995) 1–14.

[29] M. J. Castro Diaz, E. D. Fernandez-Nieto, A class of computationally fast first order finite volume solvers: PVM methods, SIAM Journal on Scientific Computing 34 (2012) 173–196.

[30] M. Castro, J. M. Gallardo, C. Parés, High order finite volume schemes based on reconstruction of states for solving hyperbolic systems with nonconservative products. Applications to shallow-water systems, Mathematics of Computation 75 (2006) 1103–1135.

[31] S. Gottlieb, C.-W. Shu, Total variation diminishing Runge-Kutta schemes, Mathematics of Computation of the American Mathematical Society 67 (1998) 73–85.

[32] M. J. Castro, J. A. García-Rodríguez, J. M. González-Vida, C. Parés, Solving shallow-water systems in 2D domains using Finite Volume methods and multimedia SSE instructions, Journal of Computational and Applied Mathematics 221 (2008) 16–32.

[33] I. Cravero, M. Semplice, G. Visconti, Optimal definition of the nonlinear weights in multidimensional central Wenoz reconstructions, SIAM Journal on Numerical Analysis 57 (2019) 2328–2358.

[34] M. J. Castro, A. M. Ferreiro Ferreiro, J. A. García-Rodríguez, J. M. González-Vida, J. MacíAs, C. Parés, M. Elena Vázquez-Cendón, The numerical treatment of wet/dry fronts in shallow flows: Application to one-layer and two-layer systems, Mathematical and Computer Modelling 42 (2005) 419–439.

[35] A. Kurganov, G. Petrova, A second-order well-balanced positivity preserving central-upwind scheme for the Saint-Venant system, Communications in Mathematical Sciences 5 (2007) 133–160.

[36] M. Kazolea, A. I. Delis, C. E. Synolakis, Numerical treatment of wave breaking on unstructured finite volume approximations for extended Boussinesq-type equations, Journal of Computational Physics 271 (2014) 281–305.

[37] M. Ricchiuto, A. G. Filippini, Upwind residual discretization of enhanced Boussinesq equations for wave propagation over complex bathymetries, Journal of Computational Physics 271 (2014) 306–341.

[38] P. A. Madsen, H. B. Bingham, H. A. Schäffer, Boussinesq-type formulations for fully nonlinear and extremely dispersive water waves: Derivation and analysis, Proceedings of the Royal Society A: Mathematical, Physical and Engineering Sciences 459 (2003) 1075–1104.

[39] J. Macías, M. J. Castro, C. Escalante, Performance assessment of the Tsunami-HySEA model for NTHMP tsunami currents benchmarking. Laboratory data, Coastal Engineering 158 (2020).

[40] S. Beji, J. A. Battjes, Numerical simulation of nonlinear wave propagation over a bar, Coastal Engineering 23 (1994) 1–16.

[41] C. E. Synolakis, The runup of solitary waves, Journal of Fluid Mechanics 185 (1987) 523–545.

[42] J. L. Hammack, A note on tsunamis: Their generation and propagation in an ocean of uniform depth, Journal of Fluid Mechanics 60 (1973) 769–799.

[43] D. R. Fuhrman, P. A. Madsen, Tsunami generation, propagation, and run-up with a high-order Boussinesq model, Coastal Engineering 56 (2009) 747–758.